Unveiling Initial State Fluctuation Using $[p_T]$ Cumulants with ATLAS

Somadutta Bhatta

Stony Brook University

Relativistic Heavy-Ion Collisions

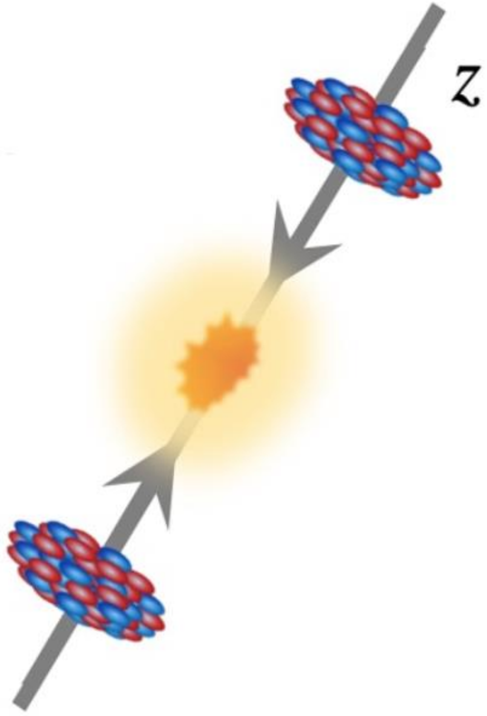

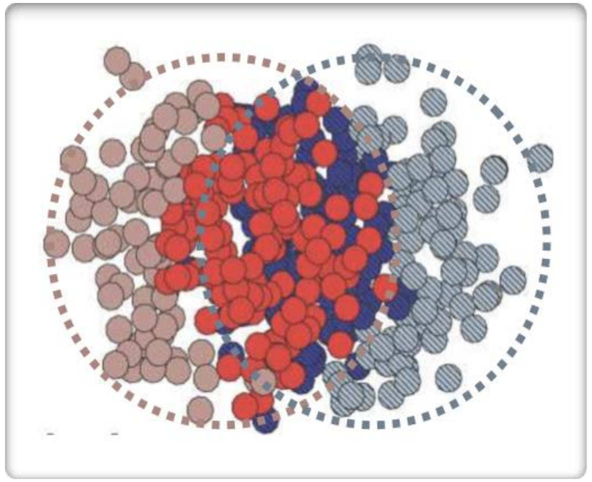

Initial State

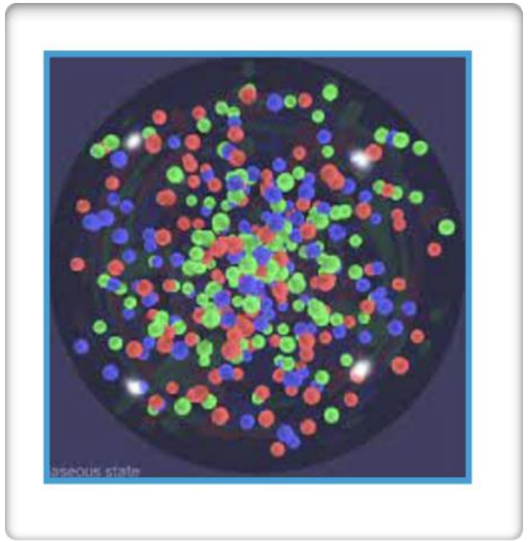

QGP

Hadronization, Free streaming

$$\frac{d^2N}{d\phi dp_T} = N(p_T)\left(\Sigma_n V_n e^{-in\phi}\right)$$

Radial Flow — Harmonic Flow

- ➢ Constraining QGP properties important to understand its phase transition into hadronic matter.
- ➢ Experimentally, QGP properties ‘inferred’ from observables measured using final-state particles.

Understanding Initial State

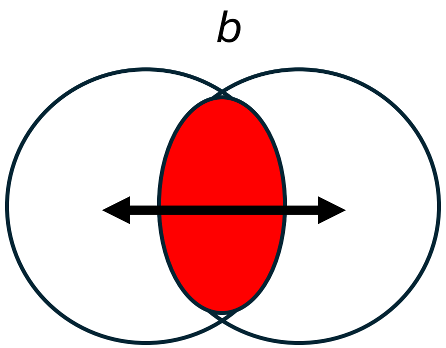

$R_\perp^2 \propto \langle r_\perp^2 \rangle$ $\varepsilon_n \propto \langle r_\perp^n e^{in\phi} \rangle$

Size **Shape**

Giacalone, 2101.00168

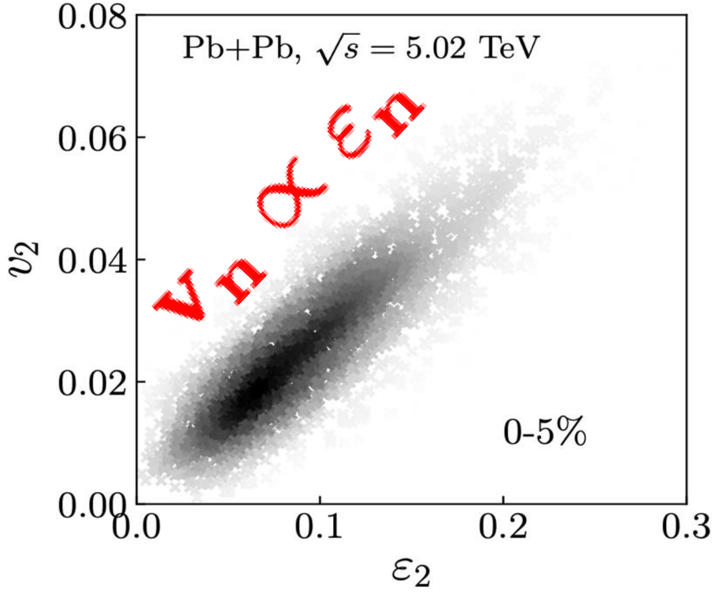

Giacalone et. al, PRC 103, 024909 (2021)

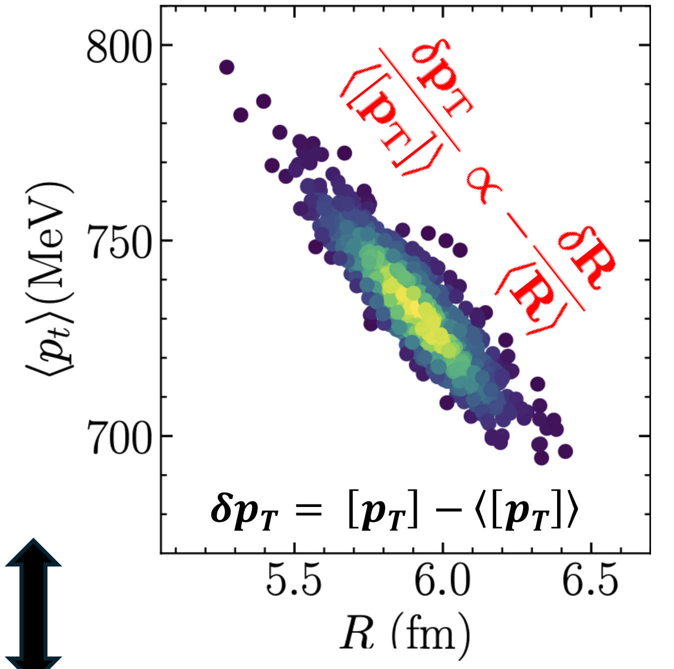

- Typically, Initial state and medium properties constrained via Bayesian analysis.

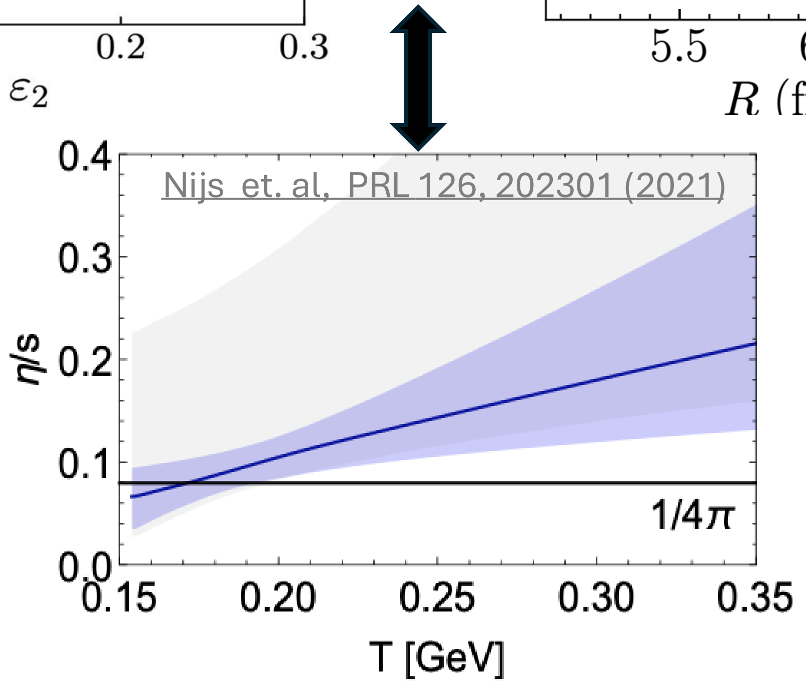

Understanding Initial State

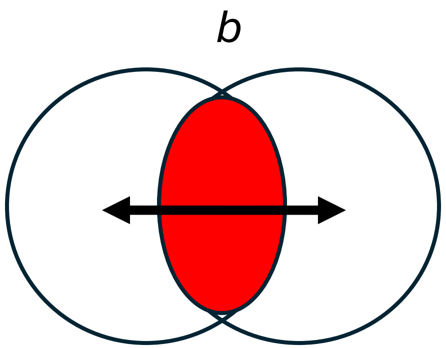

$R_\perp^2 \propto \langle r_\perp^2 \rangle$ $\varepsilon_n \propto \langle r_\perp^n e^{in\phi} \rangle$

Size **Shape**

Giacalone, 2101.00168

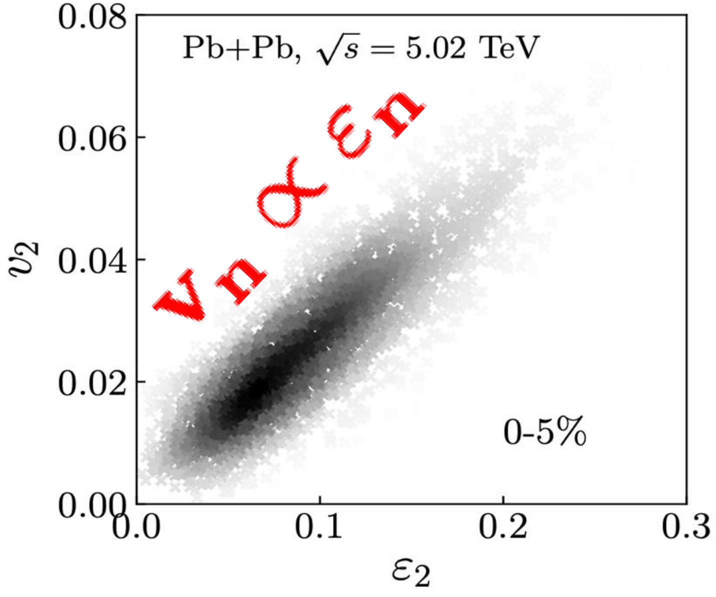

Giacalone et. al, PRC 103, 024909 (2021)

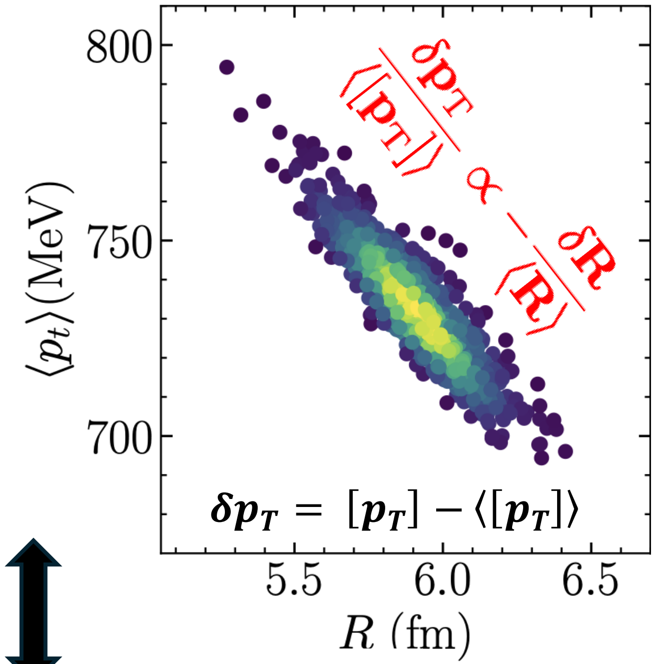

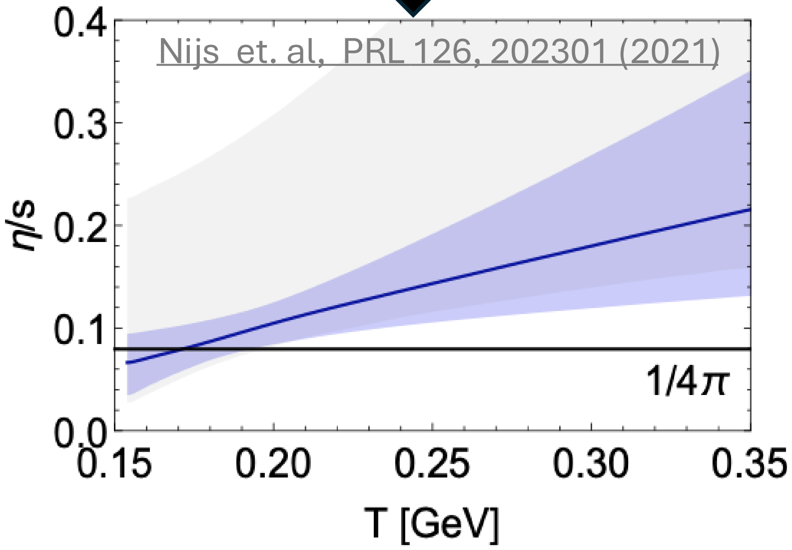

- Typically, Initial state and medium properties constrained via Bayesian analysis.
- Characterization of initial state largest source of uncertainties in extracted QGP properties.
- Flow and its fluctuations are extensively used, $[p_T]$ *Fluctuations less leveraged*.

History : Components of p_T from particle spectra

- For radially expanding medium at temperature T, total energy (non-relativistic)

$$E_{tot} = E_{th}(T_{kin}) + \frac{1}{2}m\beta^2$$

Where, T_{kin}: Freezeout temperature (Kinetic). **Thermal motion**

β : Radial-Flow velocity of the surface of source. **Collective Radial Flow**

- **Final State p_T** arises from a combination of contributions from **Radial Flow** as well as **Thermal motion of particles.**

- Traditionally, β, T_{kin} extracted by simultaneous Blast-Wave fits to p_T spectra of identified hadrons.

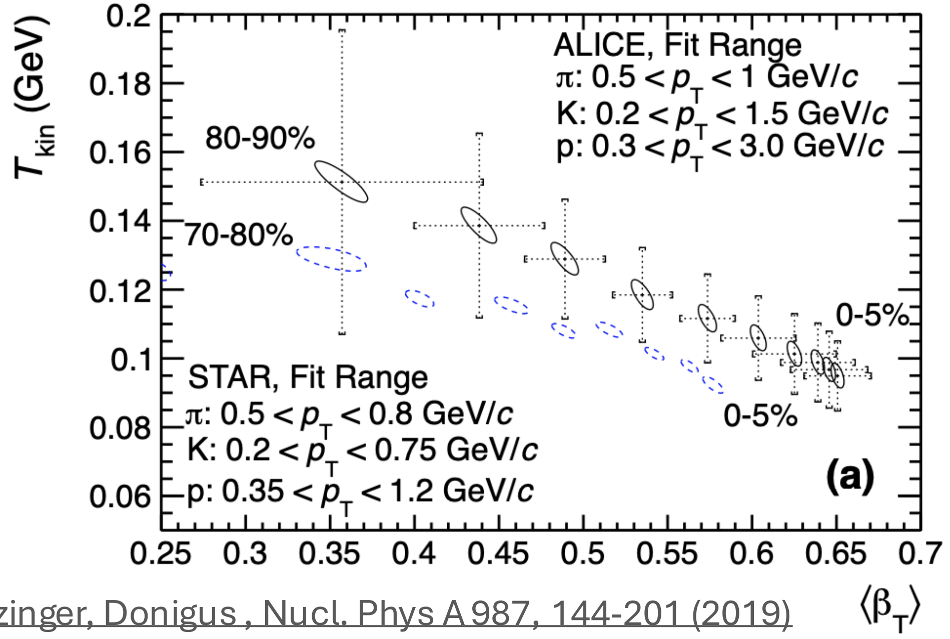

Munzinger, Donigus , Nucl. Phys A 987, 144-201 (2019)

History : Components of p_T from particle spectra

- For radially expanding medium at temperature T, total energy (non-relativistic)

$$E_{tot} = E_{th}(T_{kin}) + \frac{1}{2}m\beta^2$$

Where, T_{kin}: Freezeout temperature (Kinetic). **Thermal motion**

β : Radial-Flow velocity of the surface of source. **Collective Radial Flow**

- **Final State p_T** arises from a combination of contributions from **Radial Flow** as well as **Thermal motion of particles.**

- Traditionally, β, T_{kin} extracted by simultaneous Blast-Wave fits to p_T spectra of identified hadrons.

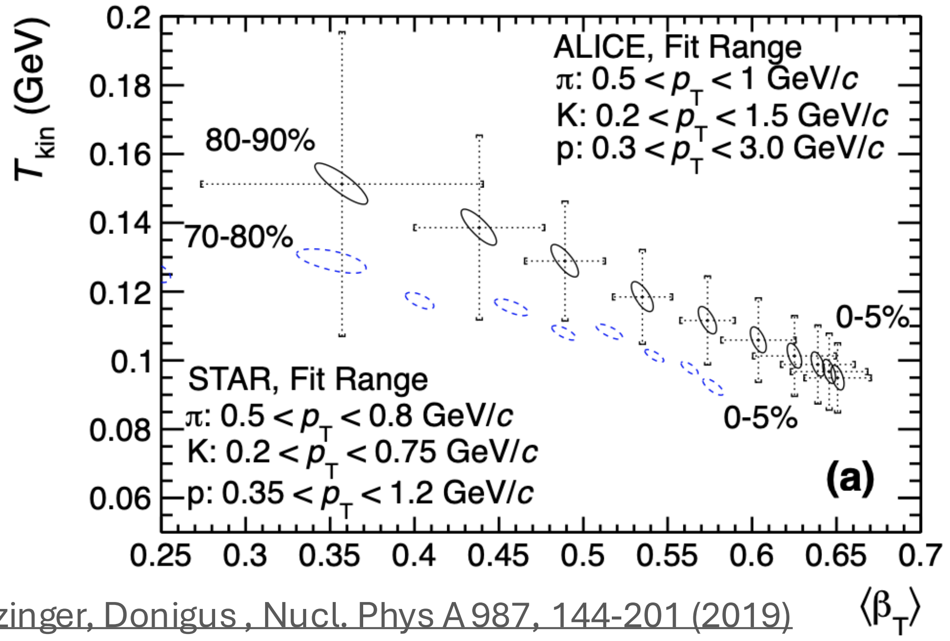

Munzinger, Donigus , Nucl. Phys A 987, 144-201 (2019)

- Effectively provides average value of β and T_{kin}.
- Does not capture `Event-by-Event' fluctuations in initial state geometry or energy deposition.

New Model to Disentangle Components of $[p_T]$

- On an event-by event basis, categorize two sources of fluctuations influencing final state measured $\langle[p_T]\rangle$

Giacalone et. al, PRC 103, 024909 (2021)

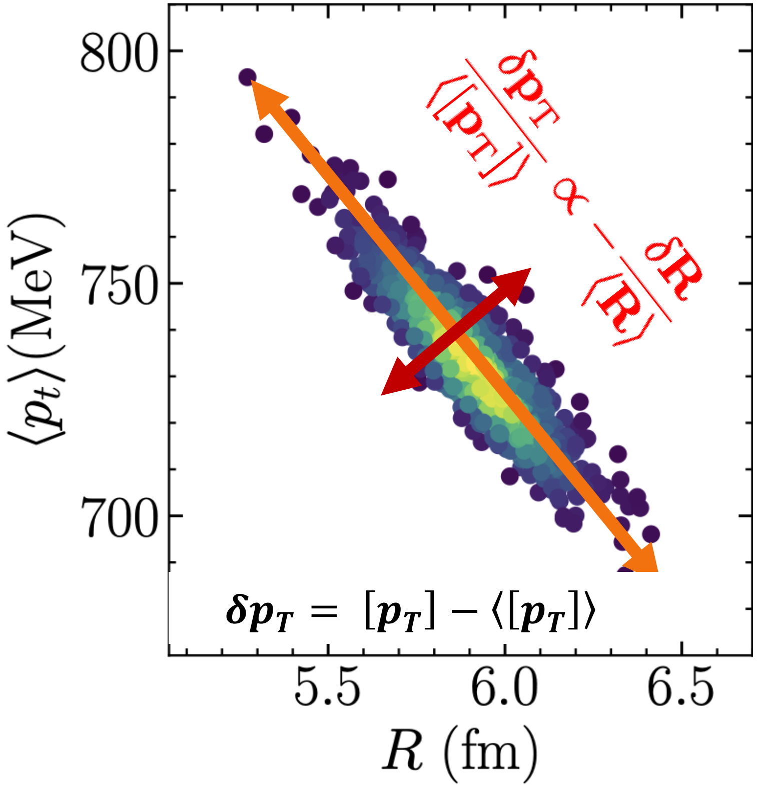

Geometrical:
Hydrodynamic response to the size fluctuations

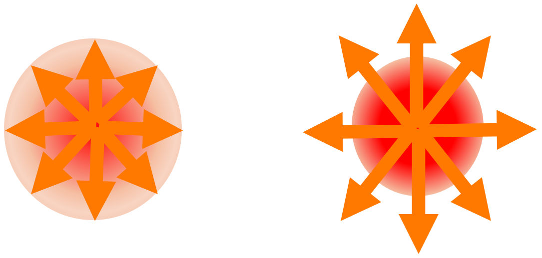

"Geometrical Component"

Intrinsic:
Fluctuations arising from Initial state, medium evolution.

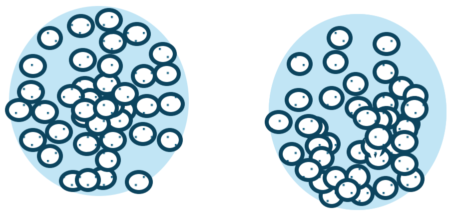

"Intrinsic Component"

Event-by-Event $[p_T]$ Fluctuations $=$ Geometrical $+$ Intrinsic

➢ Distinguishing Geometric and Intrinsic fluctuations is important to constrain both initial state and medium evolution.

New Model to Disentangle Components of $[p_T]$

2D Gaussian Model

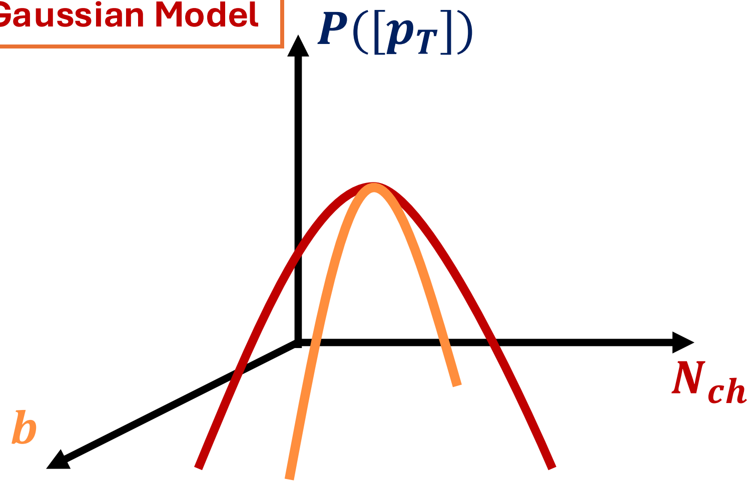

At fixed N_{ch}, b fluctuates : *Geometrical*

At fixed b, N_{ch} fluctuates: *Intrinsic*

New Model to Disentangle Components of $[p_T]$

2D Gaussian Model

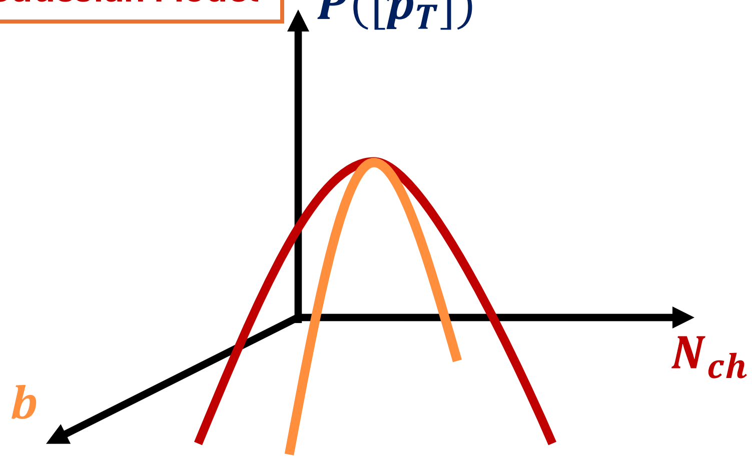

At fixed N_{ch}, b fluctuates : *Geometrical*

At fixed b, N_{ch} fluctuates: *Intrinsic*

Effect of diminishing b fluctuations with increasing N_{ch}

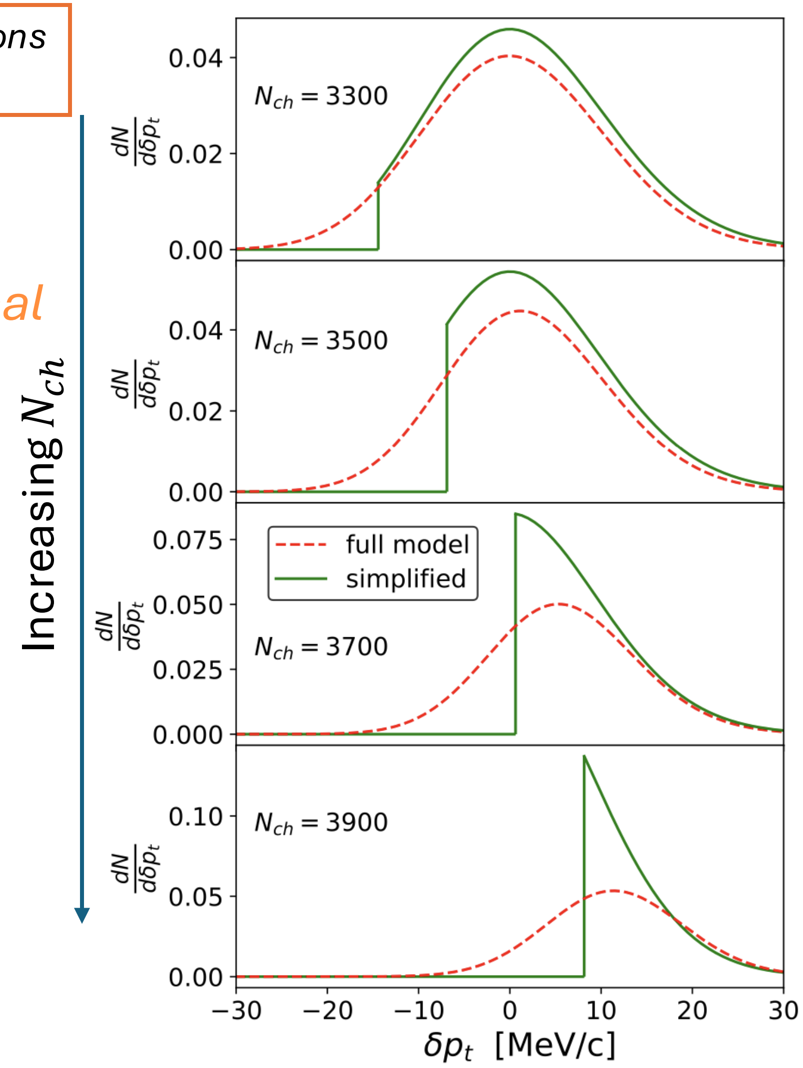

- In ultra-central collisions, b →0.
  $\Longrightarrow$ upper bound on R $\Longrightarrow$ Imposes lower bound on δp_T. $\frac{\delta p_{\mathrm{T}}}{\langle [p_{\mathrm{T}}] \rangle} \propto -\frac{\delta R}{\langle R \rangle}$

Samanta et. al, PRC108, 024908 (2023)
Samanta et. al, PRC109, L051902(2024)

New Model to Disentangle Components of $[p_T]$

2D Gaussian Model

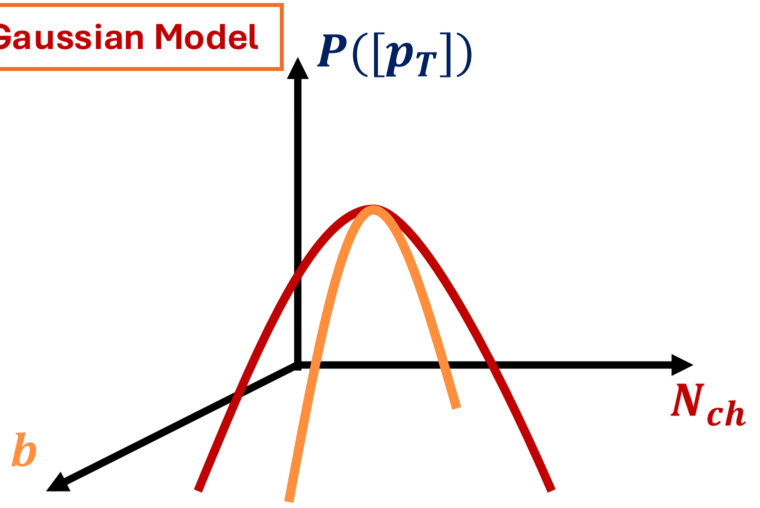

Effect of diminishing b fluctuations with increasing N_{ch}

At fixed N_{ch}, b fluctuates : *Geometrical*
At fixed b, N_{ch} fluctuates: *Intrinsic*

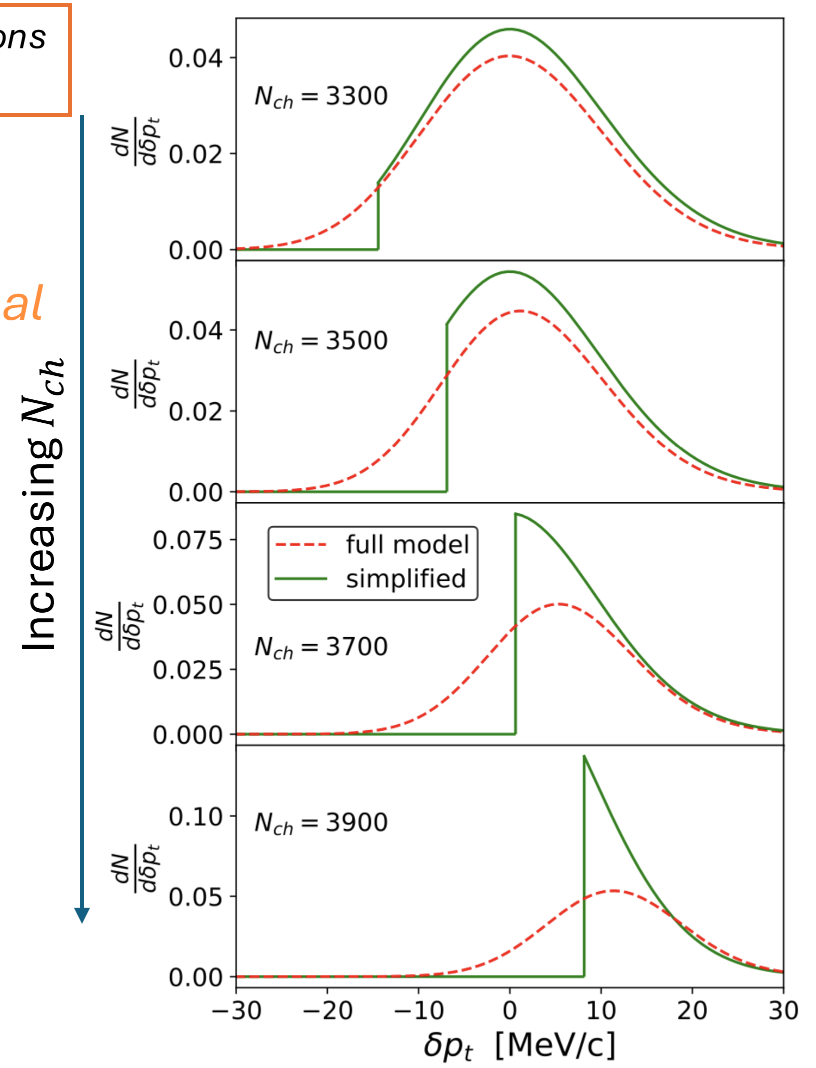

- In ultra-central collisions, b →0.
  $\Longrightarrow$ upper bound on $R \Longrightarrow$ Imposes lower bound on δp_T. $\frac{\delta p_{\mathrm{T}}}{\langle [p_{\mathrm{T}}] \rangle} \propto -\frac{\delta R}{\langle R \rangle}$

➢ With increasing N_{ch} in UCC, expect:
1. Decrease variance of $P([p_T])$,
2. Increase skewness of $P([p_T])$,
   purely due to constraints on Geometrical fluctuations,
   Intrinsic Fluctuations unhindered.

Samanta et. al, PRC108, 024908 (2023)
Samanta et. al, PRC109, L051902(2024)

Measurement of $[p_T]$ Cumulants in ATLAS

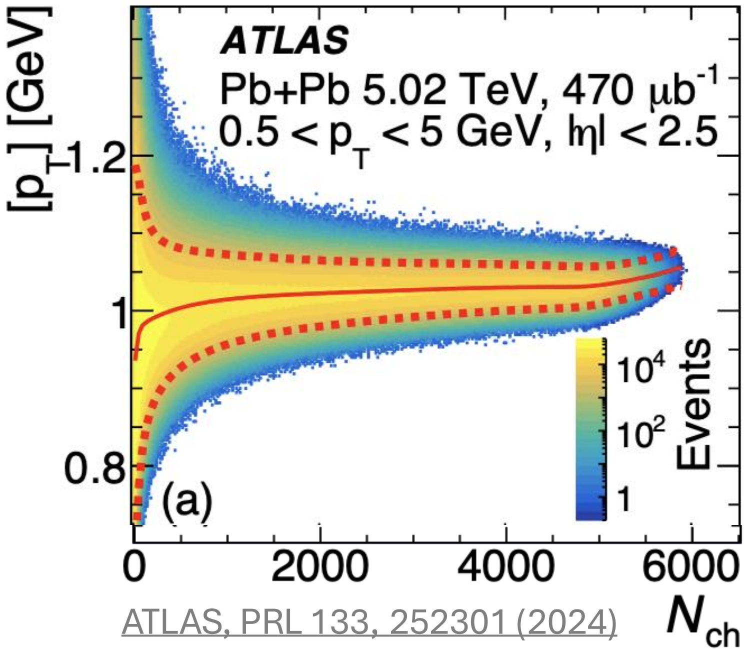

ATLAS, PRL 133, 252301 (2024)

- Use standard cumulant method used in flow analysis to measure Event by Event fluctuations in $[p_T]$:

$$c_n = \frac{\sum_{i_1 \neq \ldots . \neq i_n} w_{i_1} .. w_{i_n} (p_{\mathrm{T},i_1} - \langle [p_\mathrm{T}] \rangle) \ldots (p_{\mathrm{T},i_n} - \langle [p_\mathrm{T}] \rangle)}{\sum_{i_1 \neq \ldots . \neq i_n} w_{i_1} \ldots w_{i_n}}$$

- Variance, $\langle c_2 \rangle$ and skewness, $\langle c_3 \rangle$ are further normalized to obtain dimensionless quantities

$$k_2 = \frac{\langle c_2 \rangle}{\langle [p_\mathrm{T}] \rangle^2}$$

Scaled Variance

$$k_3 = \frac{\langle c_3 \rangle}{\langle [p_\mathrm{T}] \rangle^3}$$

Scaled Skewness

$$\gamma = \frac{\langle c_3 \rangle}{\langle c_2 \rangle^{3/2}}$$

Normalized Skewness

Measurement of $[p_T]$ Cumulants in ATLAS

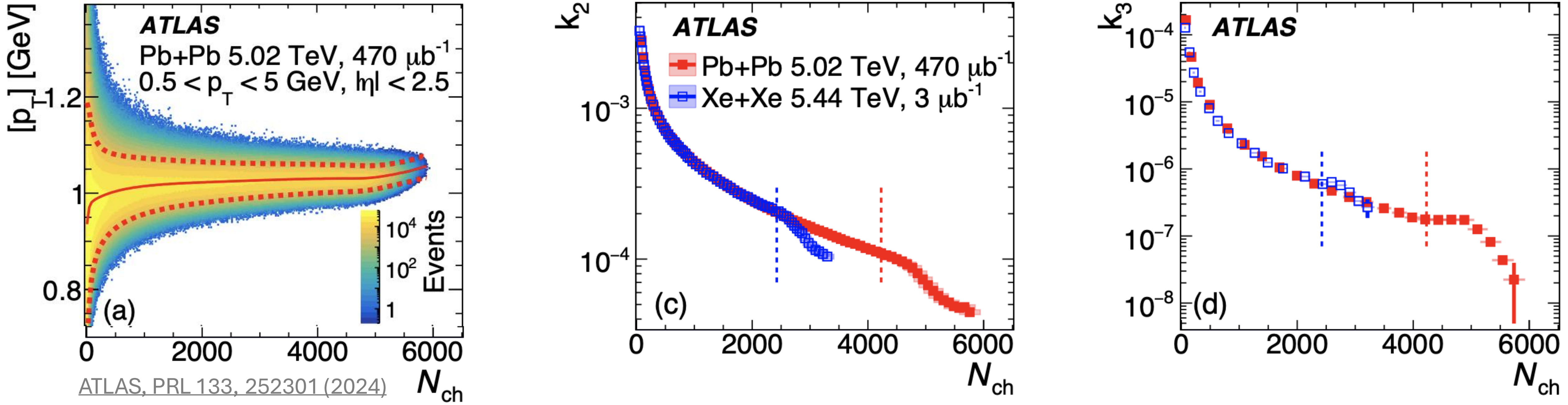

ATLAS, PRL 133, 252301 (2024)

- Use standard cumulant method used in flow analysis to measure Event by Event fluctuations in $[p_T]$:

$$c_n = \frac{\sum_{i_1 \neq ....\neq i_n} w_{i_1}..w_{i_n}(p_{\mathrm{T},i_1} - \langle [p_{\mathrm{T}}]\rangle)...(p_{\mathrm{T},i_n} - \langle [p_{\mathrm{T}}]\rangle)}{\sum_{i_1 \neq ....\neq i_n} w_{i_1}...w_{i_n}}$$

- Variance, $\langle c_2 \rangle$ and skewness, $\langle c_3 \rangle$ are further normalized to obtain dimensionless quantities

$$k_2 = \frac{\langle c_2 \rangle}{\langle [p_{\mathrm{T}}] \rangle^2}$$

Scaled Variance

$$k_3 = \frac{\langle c_3 \rangle}{\langle [p_{\mathrm{T}}] \rangle^3}$$

Scaled Skewness

$$\gamma = \frac{\langle c_3 \rangle}{\langle c_2 \rangle^{3/2}}$$

Normalized Skewness

Measurement of $[p_T]$ Cumulants in ATLAS

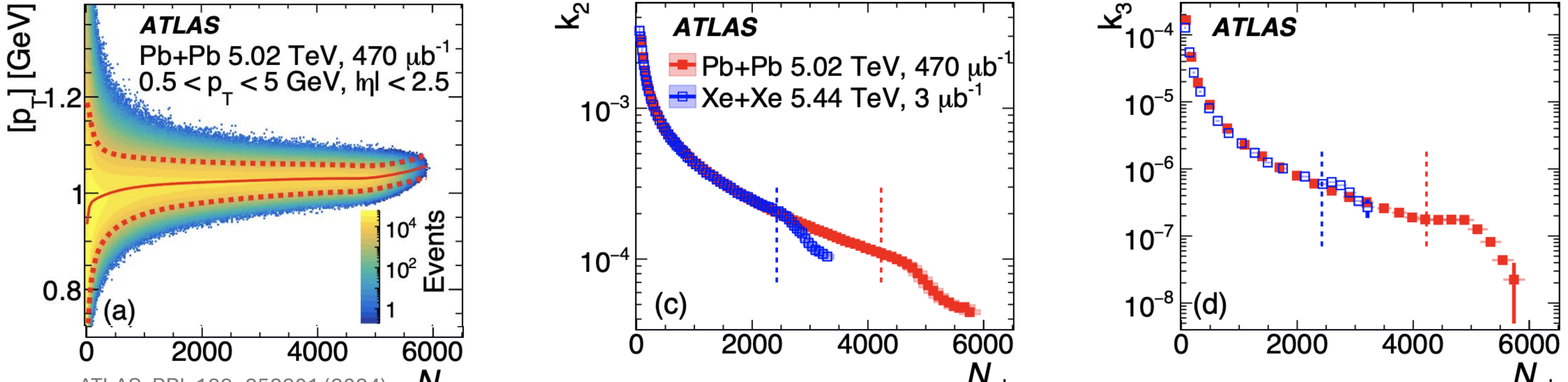

ATLAS, PRL 133, 252301 (2024)

➢ Measured k_n approximately follow power-law dependence with N_{ch}.

Bhatta, et. al, PRC 105, 024904 (2022)

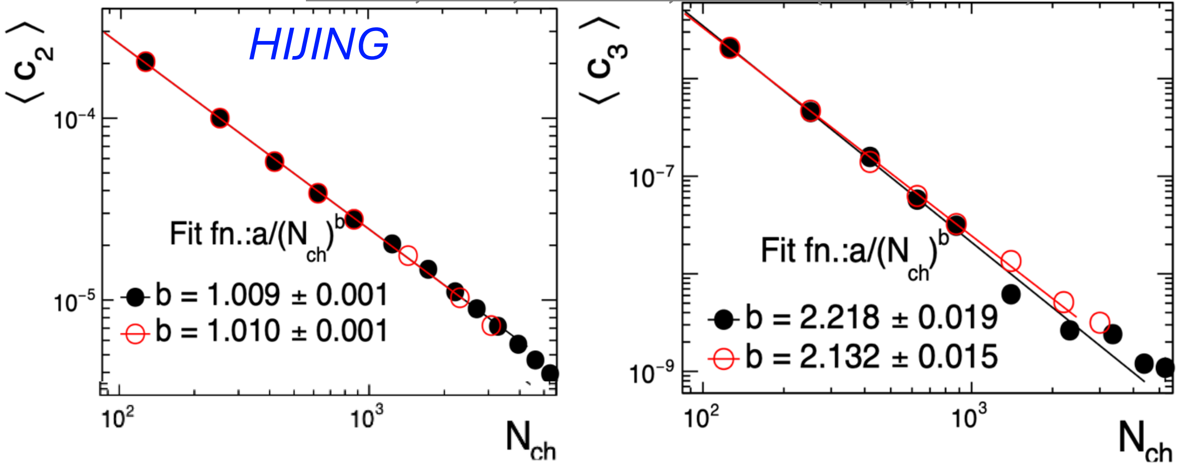

- *Independent Superposition Scenario:*
  $\langle c_2 \rangle \propto {}^{1}/_{N_{ch}}, \quad \langle c_3 \rangle \propto ({}^{1}/_{N_{ch}})^2$

➢ Explains approximate power-law dependence of k_n with N_{ch}.

Measurement of $[p_T]$ Cumulants in ATLAS

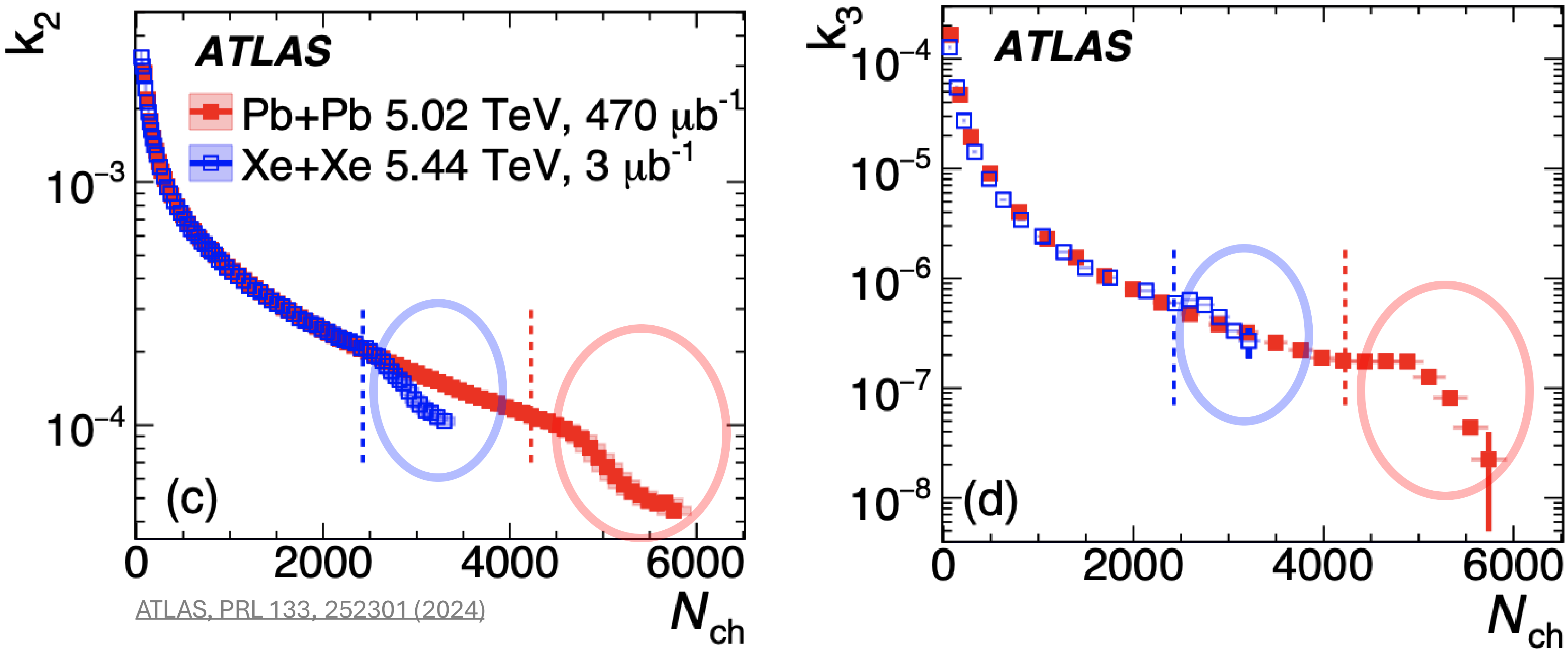

ATLAS, PRL 133, 252301 (2024)

- In UCC, (after N_{ch} corresponding to 5% Centrality),
  - A sharp drop is observed for k_2,
  - A small rise followed by drop is observed for k_3.
- Expected from narrowing of Geometrical fluctuations as $b \to 0$

Constraining Geometrical and Intrinsic Fluctuations

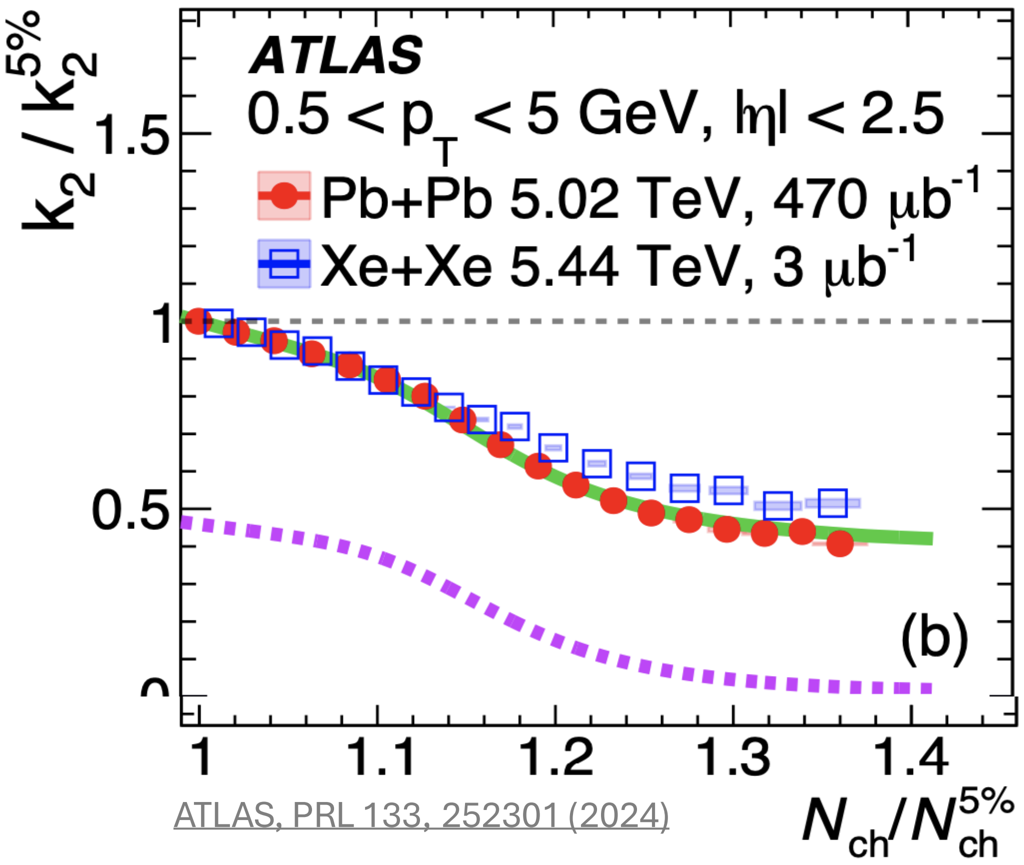

ATLAS, PRL 133, 252301 (2024)

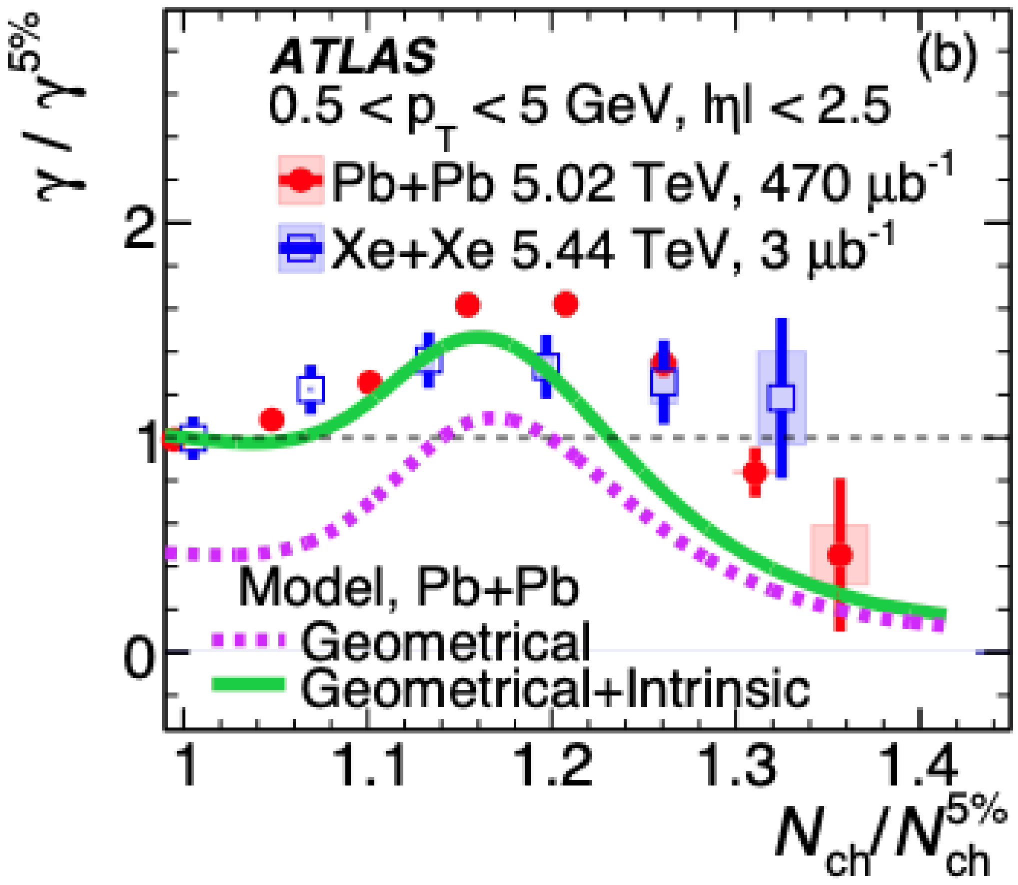

$[p_T]$ **Fluctuations** $=$ **Geometrical** $+$ **Intrinsic**

- In Ultra-Central Collisions:
  1. Fall of k_2 explained entirely by diminishing variance of Geometrical fluctuations.
  2. Increase in γ due to truncation of distribution of event-wise $[p_T]$.

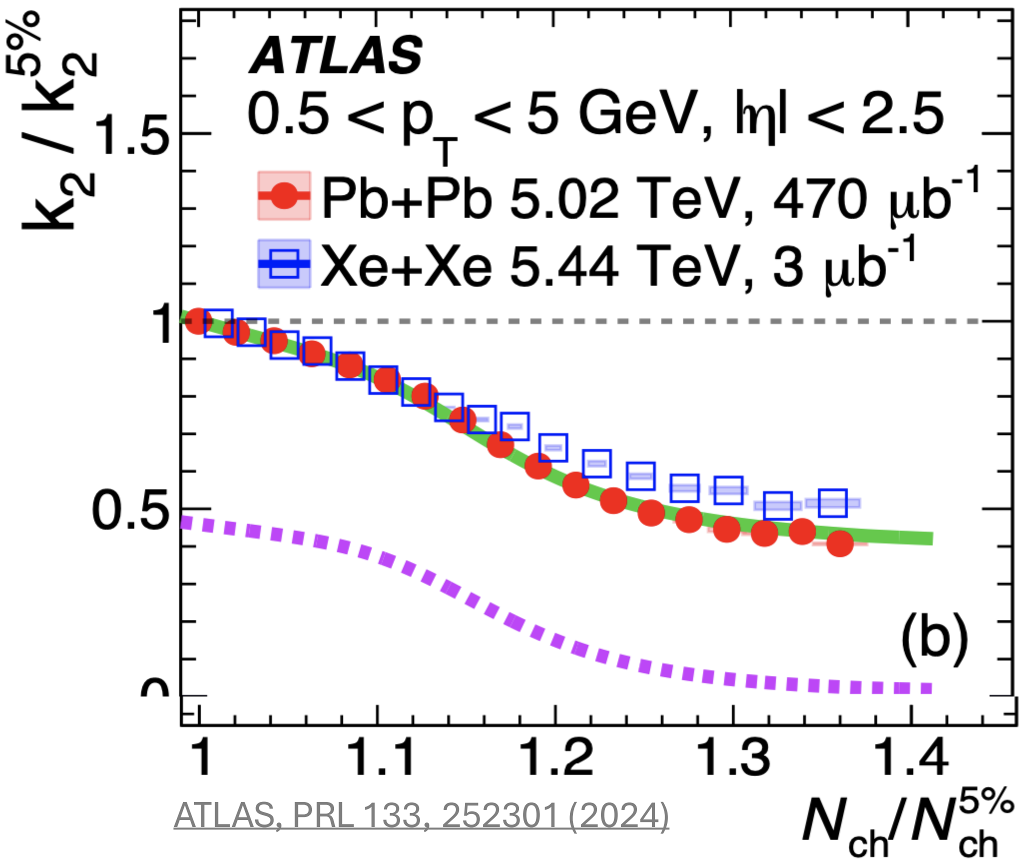

ATLAS, PRL 133, 252301 (2024)

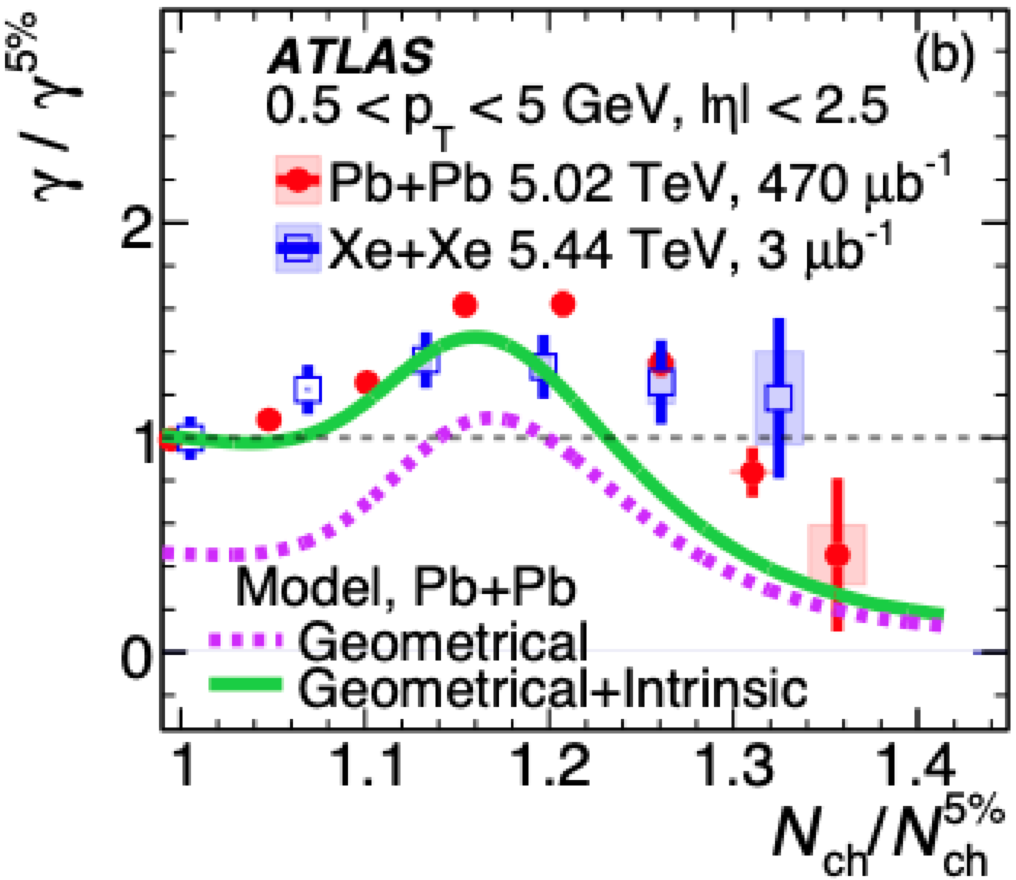

$[p_T]$ **Fluctuations** $=$ **Geometrical** $+$ **Intrinsic**

- Experimental measurement of the cumulants of $P([p_T])$ is effective towards disentangling "*Geometrical* fluctuations" from "*Intrinsic* fluctuations" in HIC.

Constraining c_S^2 using $\langle[p_T]\rangle$

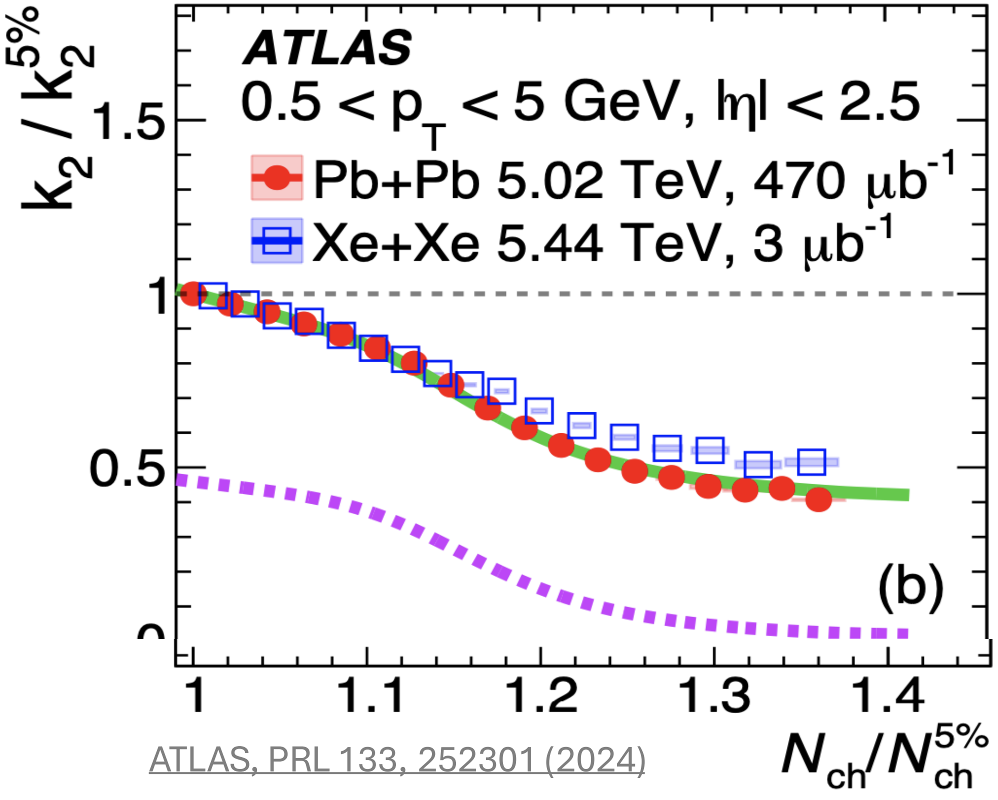

ATLAS, PRL 133, 252301 (2024)

- In UCC, $b \to 0$, evident from gradual narrowing of k_2.

Constraining c_S^2 using $\langle[p_T]\rangle$

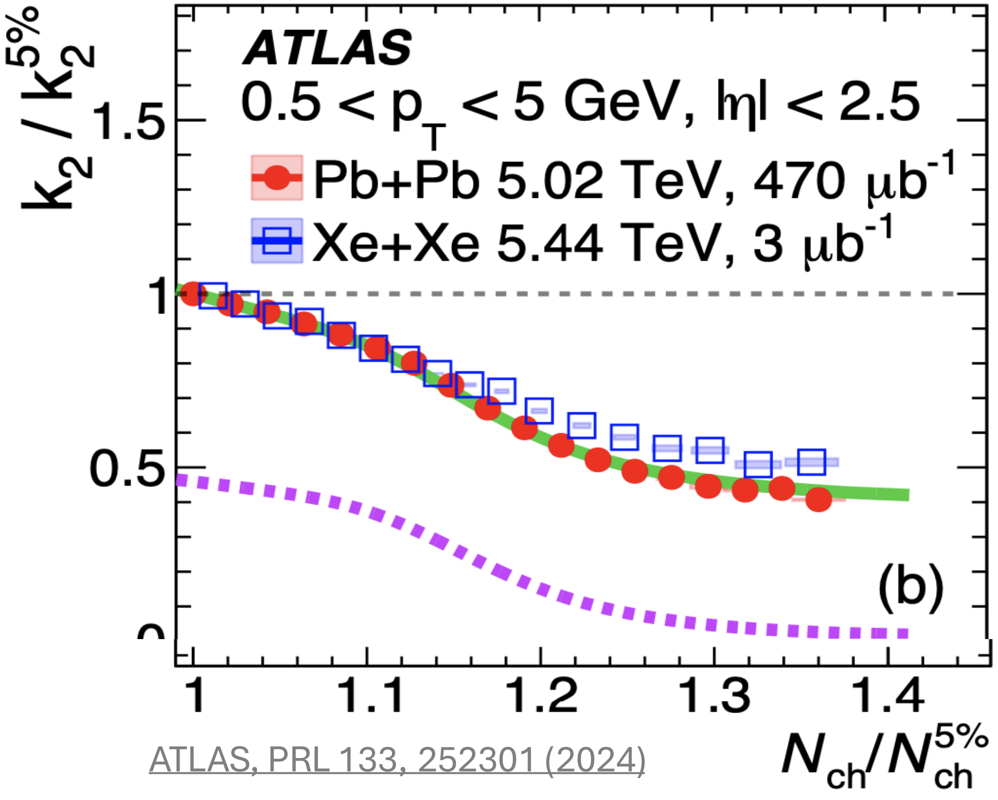

ATLAS, PRL 133, 252301 (2024)

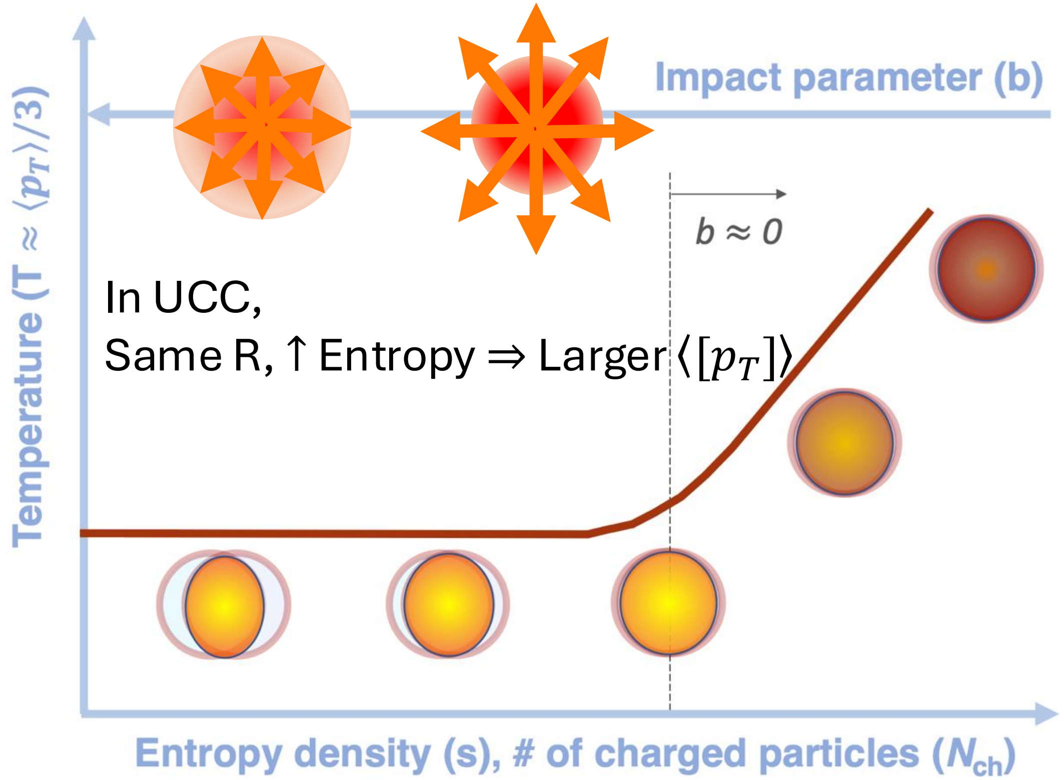

CMS, RPP 87, 077801 (2024)
Gardim et. al, PLB 809, 135749 (2020)

- In UCC, $b \to 0$, evident from gradual narrowing of k_2.
- Within approximately fixed geometry (b), selecting larger N_{ch} chooses events with larger entropy density → arising from intrinsic component.

Constraining c_S^2 using $\langle[p_T]\rangle$

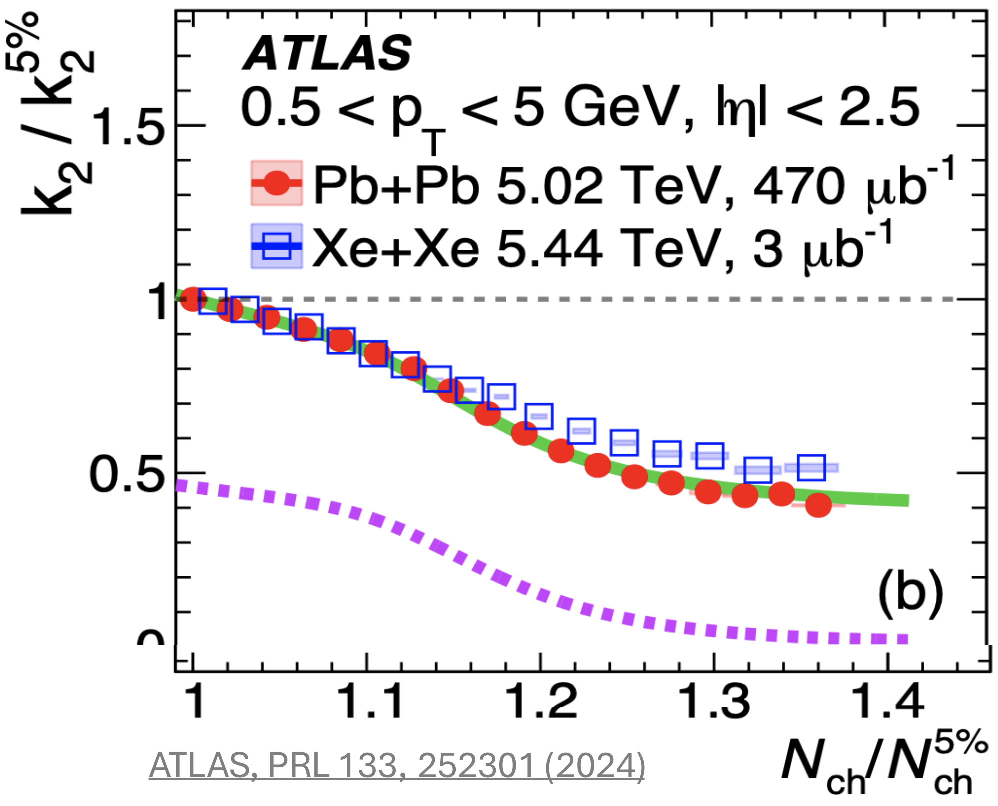

ATLAS, PRL 133, 252301 (2024)

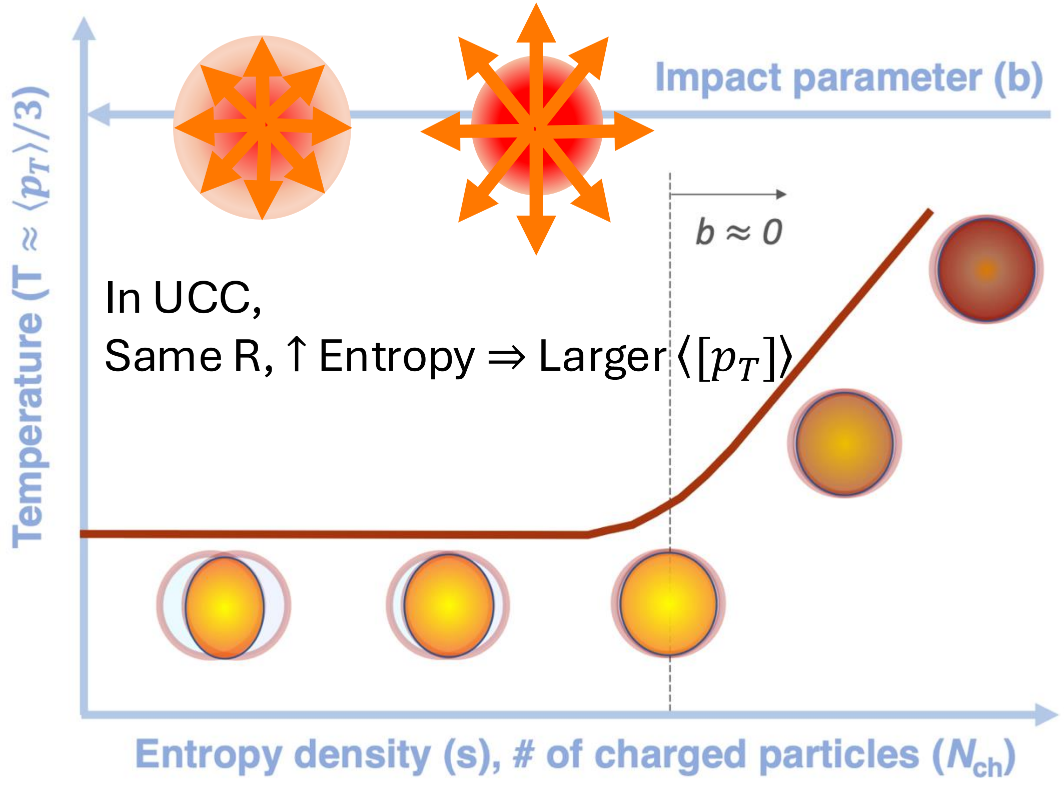

CMS, RPP 87, 077801 (2024)
Gardim et. al, PLB 809, 135749 (2020)

- In UCC, $b \to 0$, evident from gradual narrowing of k_2.
- Within approximately fixed geometry (b), selecting larger N_{ch} chooses events with larger entropy density → arising from intrinsic component.
- Larger entropy density within a fixed geometry leads to larger radial push or $\langle[p_T]\rangle$.

Constraining c_S^2 using $\langle[p_T]\rangle$

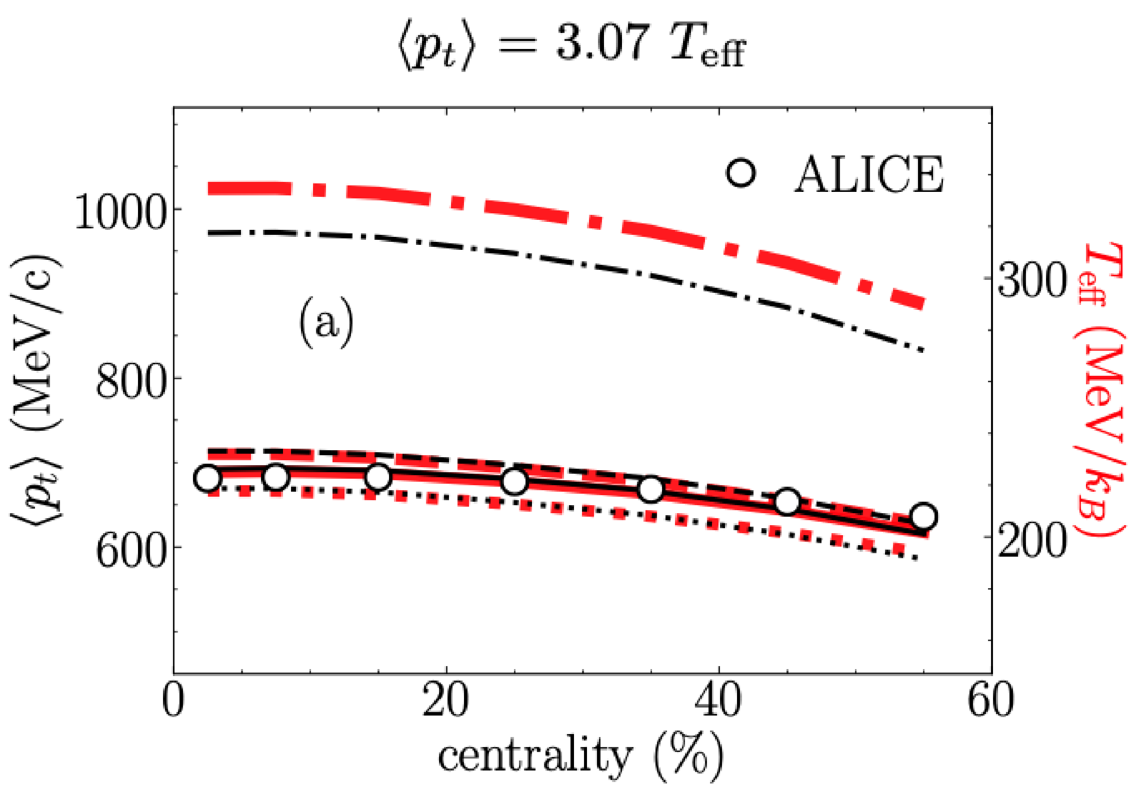

Gardim et. al, Nat. Phys 16, (2020)

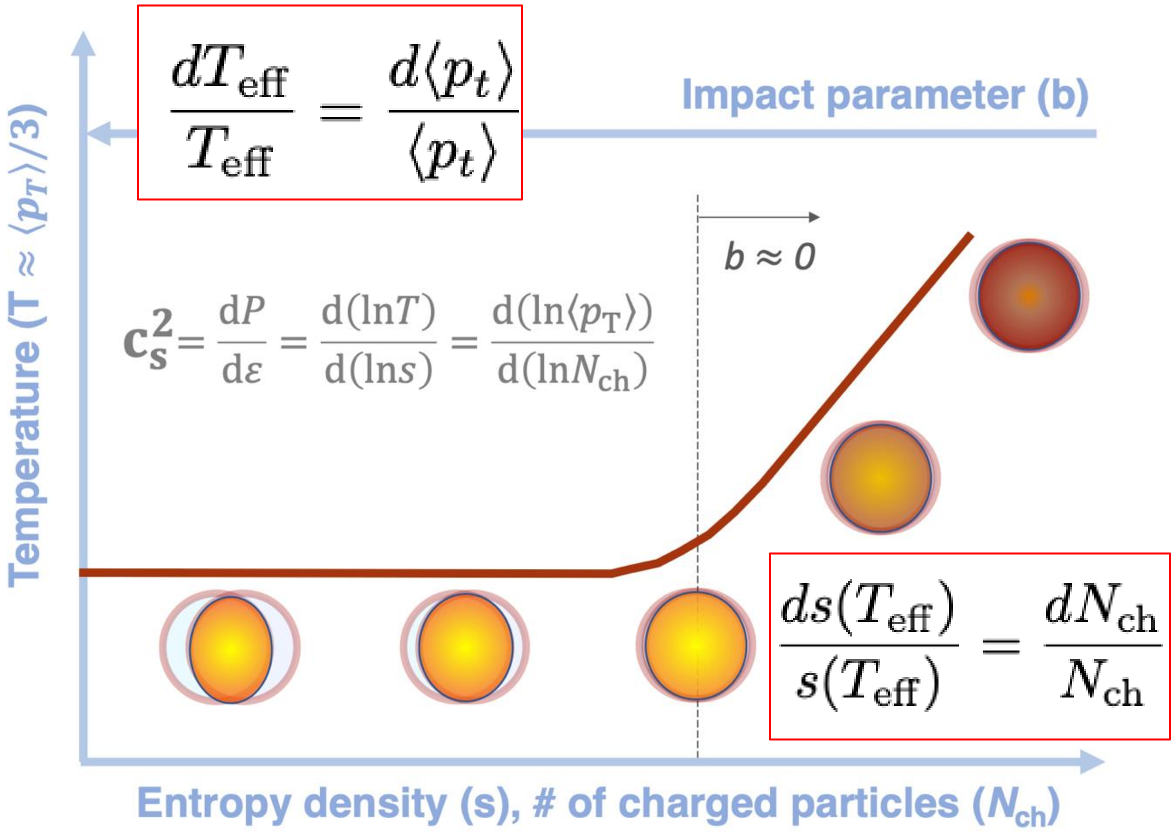

CMS, RPP 87, 077801 (2024)
Gardim et. al, PLB 809, 135749 (2020)

- The slope of this rise of $\langle[p_T]\rangle$ in UCC is related to speed of sound of QGP:

$$c_s^2 = \frac{dP}{d\epsilon} = \frac{d(lnT)}{d(lns)} = \frac{d(ln\langle p_T\rangle)}{d(lnN_{ch})}$$

Constraining c_S^2 using $\langle[p_T]\rangle$

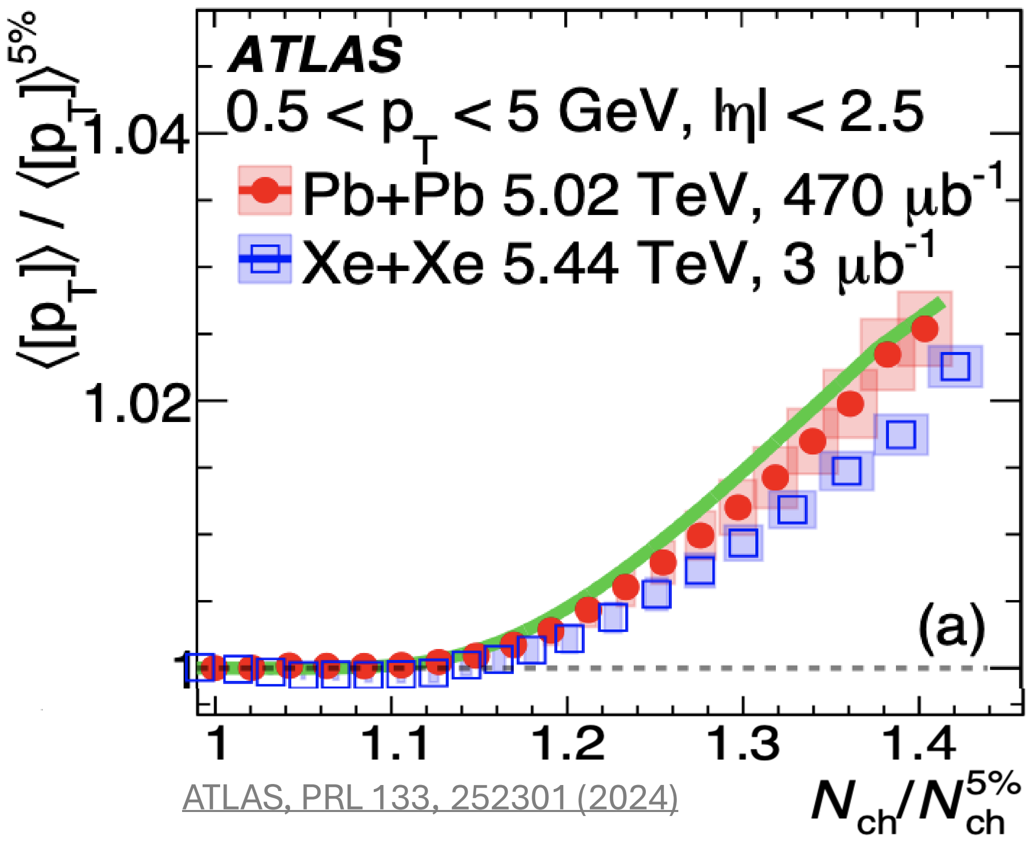

ATLAS, PRL 133, 252301 (2024)

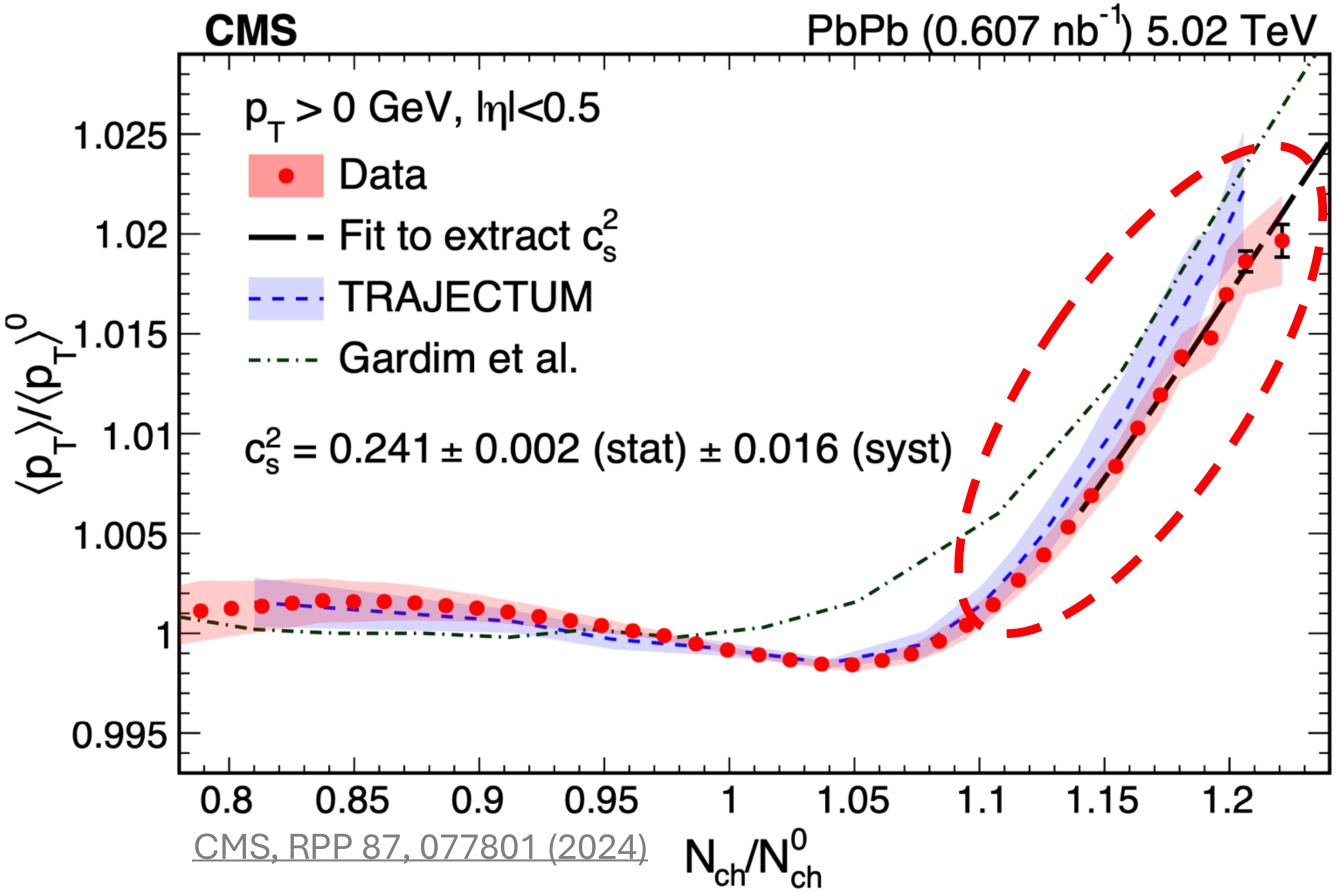

CMS, RPP 87, 077801 (2024)

- Both ATLAS and CMS have observed the steep increase in slope of $\langle[p_T]\rangle$ in UCC.
  $\Longrightarrow$ Evidence of overlap area reaching its maximum and Thermalization of system.

- CMS extracted the slope of this rise: claimed the speed of sound of QGP, c_s^2 ≈0.241.

Caveat: Dependence of UCC Slope of $\langle[p_T]\rangle$ on Evolution Dynamics

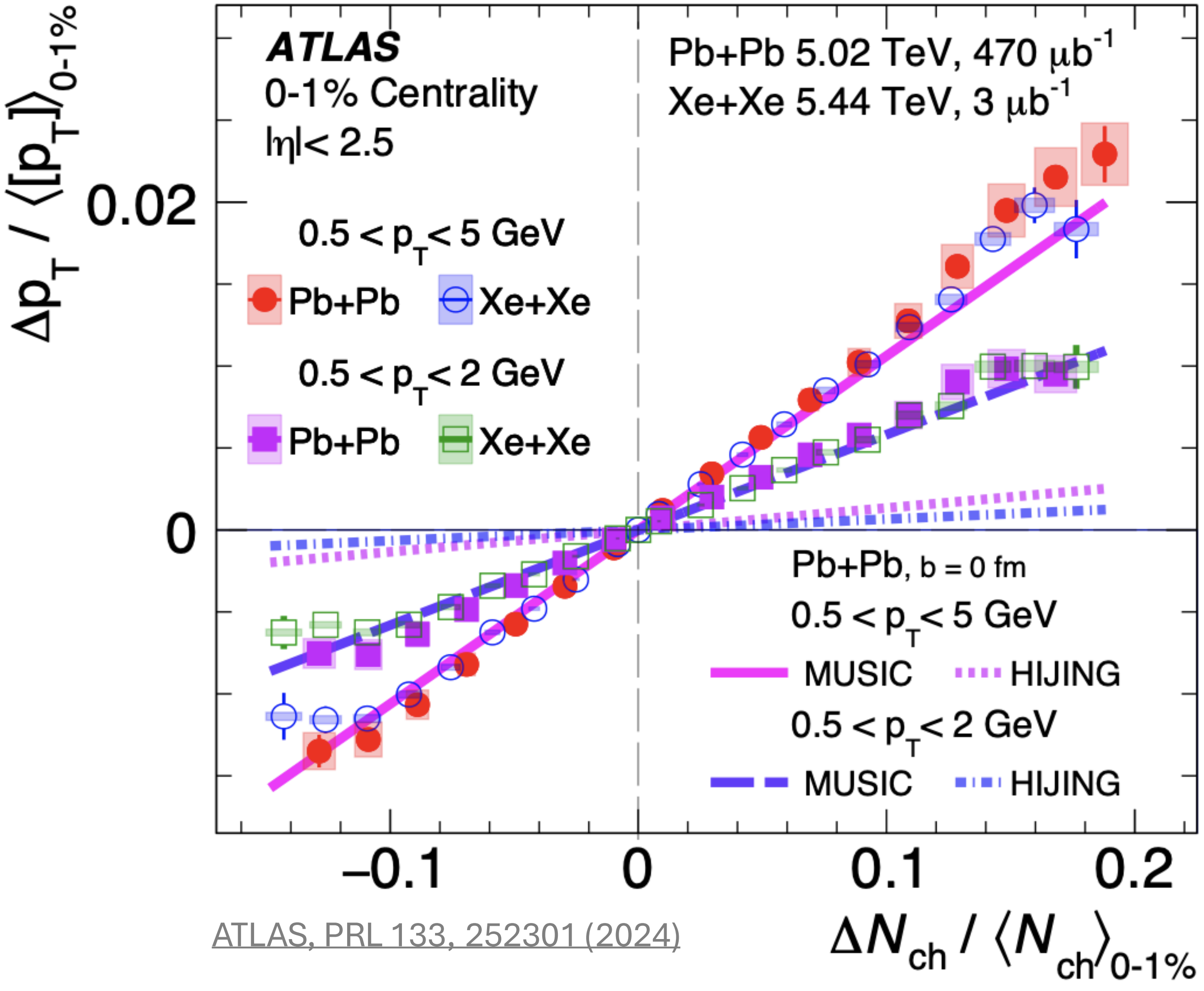

ATLAS, PRL 133, 252301 (2024)

$$c_s^2(T_{\text{eff}}) \propto \frac{d\ln(\langle[p_{\text{T}}]\rangle)}{d\ln(N_{\text{ch}}^{\text{rec}})} \approx \frac{\Delta p_{\text{T}}/\langle[p_{\text{T}}]\rangle}{\Delta N_{\text{ch}}^{\text{rec}}/\langle N_{\text{ch}}^{\text{rec}}\rangle}$$

- ATLAS: slope of this rise depends on the p_T-range of the particles.

Caveat: Dependence of UCC Slope of $\langle[p_T]\rangle$ on Evolution Dynamics

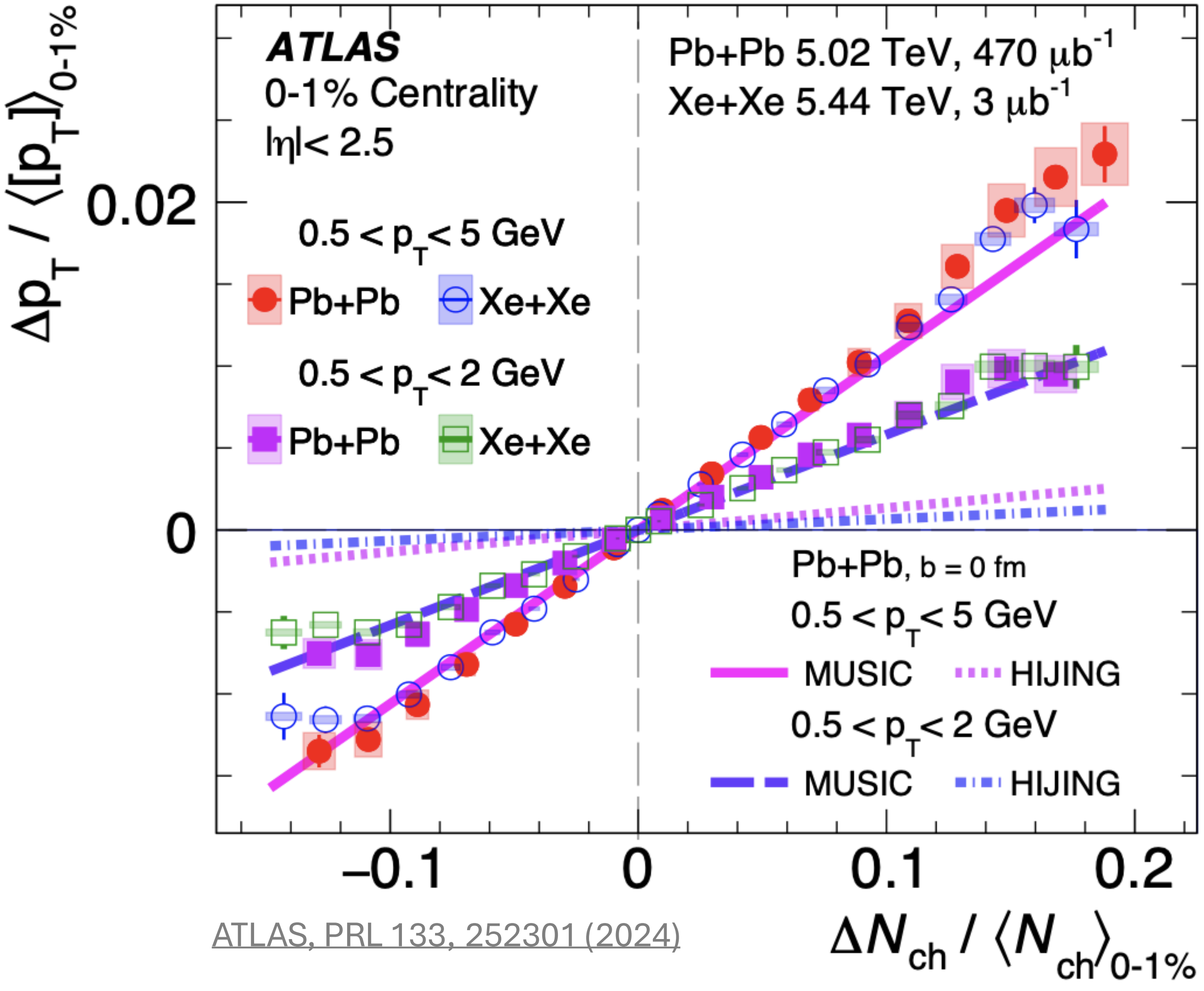

ATLAS, PRL 133, 252301 (2024)

$$c_s^2(T_{\rm eff}) \propto \frac{d\ln(\langle[p_{\rm T}]\rangle)}{d\ln(N_{\rm ch}^{\rm rec})} \approx \frac{\Delta p_{\rm T}/\langle[p_{\rm T}]\rangle}{\Delta N_{\rm ch}^{\rm rec}/\langle N_{\rm ch}^{\rm rec}\rangle}$$

- ATLAS: slope of this rise depends on the p_T-range of the particles.
- Models without hydro evolution (or mechanisms to relate initial entropy densities to number of particles) fail to describe this UCC slope.

Caveat: Dependence of UCC Slope of $\langle[p_T]\rangle$ on Evolution Dynamics

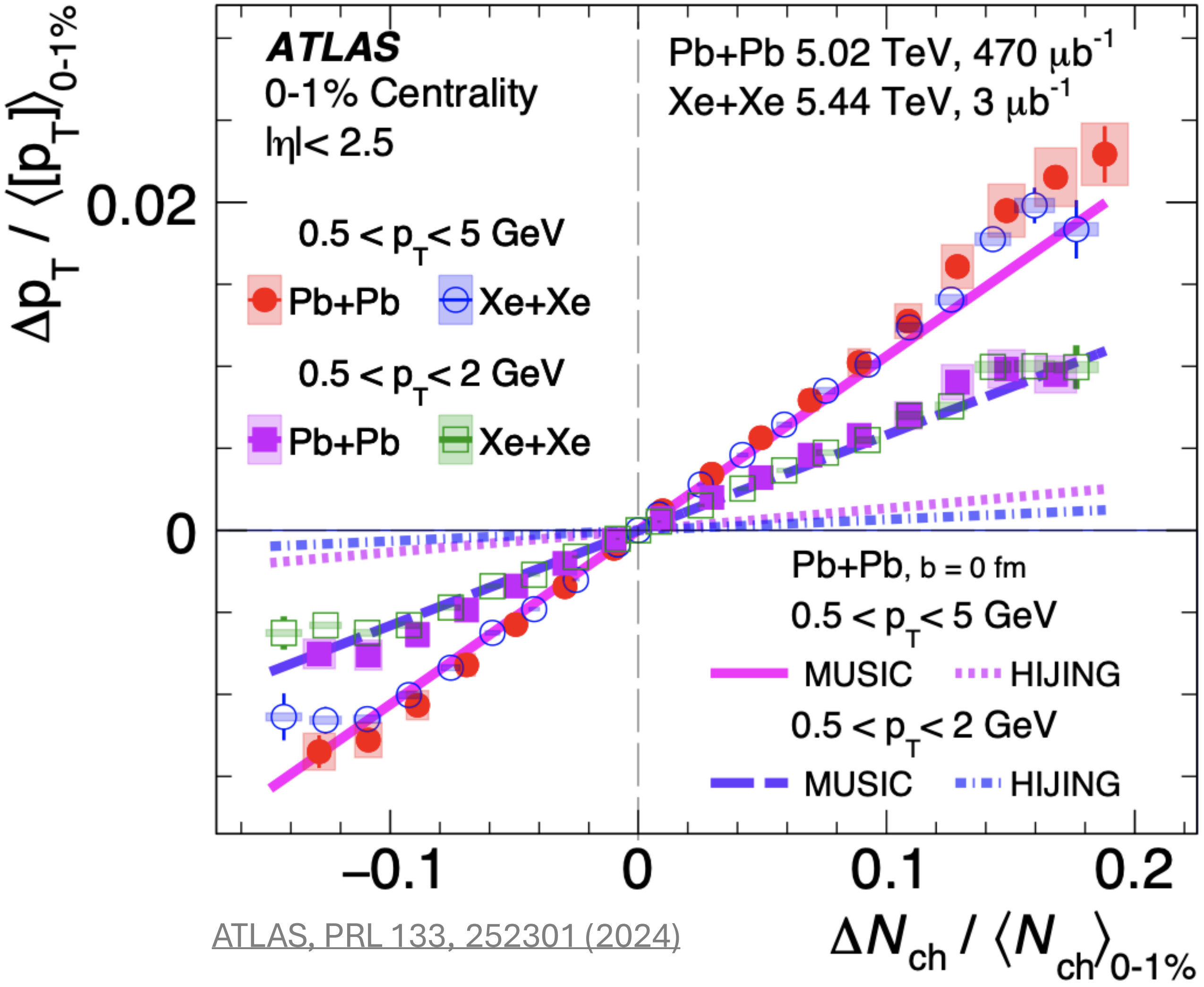

ATLAS, PRL 133, 252301 (2024)

$$c_s^2(T_{\mathrm{eff}}) \propto \frac{d\ln(\langle[p_{\mathrm{T}}]\rangle)}{d\ln(N_{\mathrm{ch}}^{\mathrm{rec}})} \approx \frac{\Delta p_{\mathrm{T}}/\langle[p_{\mathrm{T}}]\rangle}{\Delta N_{\mathrm{ch}}^{\mathrm{rec}}/\langle N_{\mathrm{ch}}^{\mathrm{rec}}\rangle}$$

- ATLAS: slope of this rise depends on the p_T-range of the particles.
- Models without hydro evolution (or mechanisms to relate initial entropy densities to number of particles) fail to describe this UCC slope.
- Slope for both p_T-ranges well described by MUSIC using $c_S^2 \approx 0.23$, corresponding to a $T_{eff} \approx 222$ MeV.

Conclusion

- Using precise measurement of $[p_T]$ cumulants in heavy-ion collisions with ATLAS, we show:

1. $[p_T]$ cumulants provide novel experimental handle to disentangle and constrain:
   Geometrical Fluctuations (Initial state overlap Size)
   Intrinsic fluctuations (Other non-geometrical sources)

2. Slope of $\langle [p_T] \rangle$ vs N_{ch} in UCC provides direct constraint on speed of sound of QGP.

Outlook I: Effect of Decorrelation on extracted c_S^2

ALICE-PUBLIC-2024-002

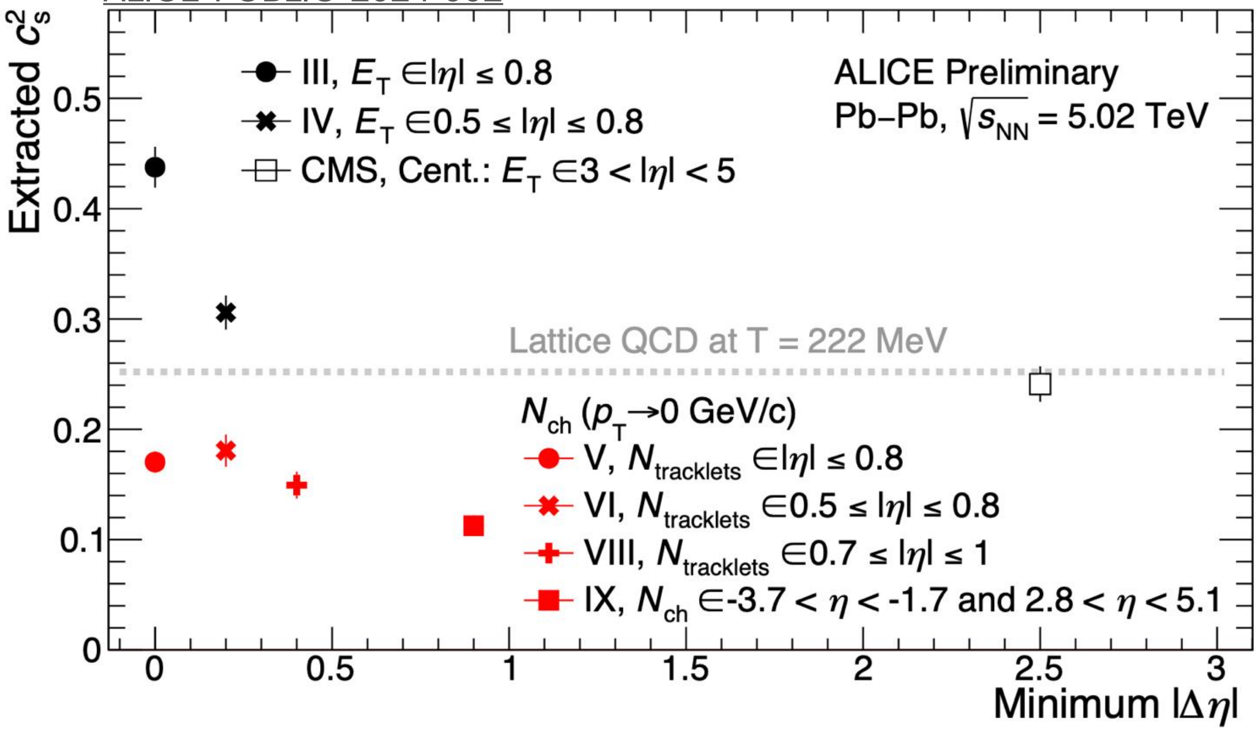

Chatterjee, Bozek, PRC 96, 014906 (2017)

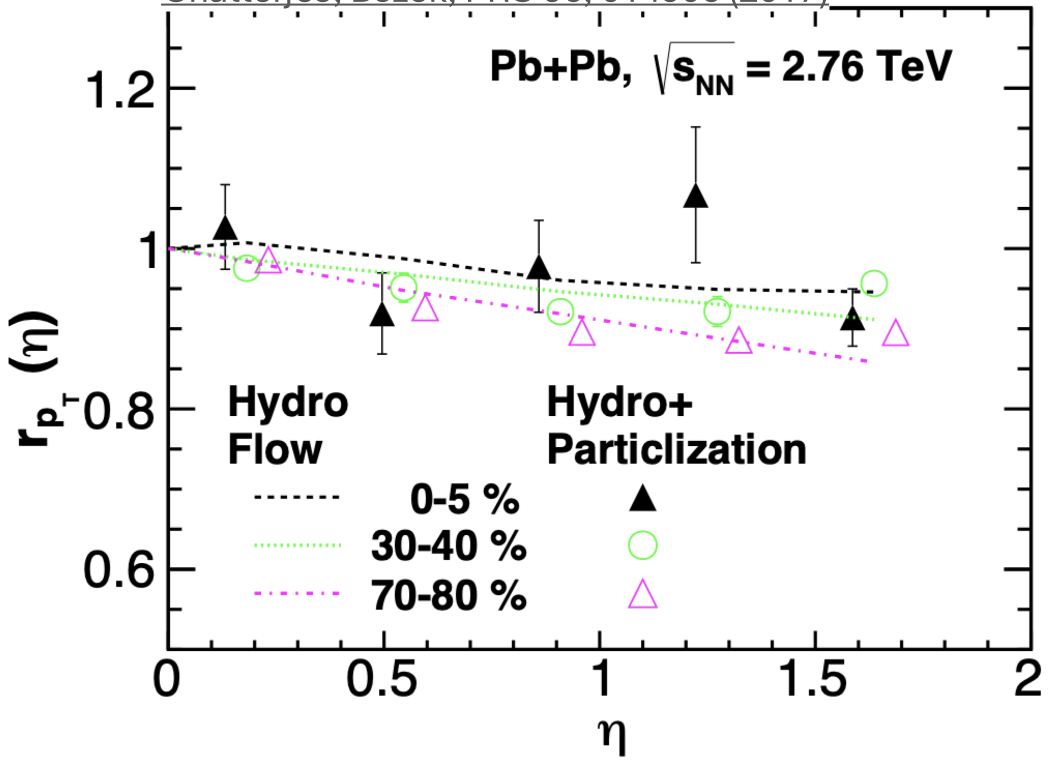

$$r_{p_T}(\eta) = \frac{\mathrm{Cov}\left([p_T]_F, [p_T]_{-\eta}\right)}{\mathrm{Cov}\left([p_T]_F, [p_T]_{\eta}\right)}$$

- Extracted c_S^2 differs between event-classification based on rapidity selection.
- Might be due to decorrelation of radial flow.
- Hydro model calculation: Radial flow displays decorrelation, just like flow decorrelations, *Better reflects longitudinal evolution of energy deposition in η.*

Outlook I: Effect of System Size

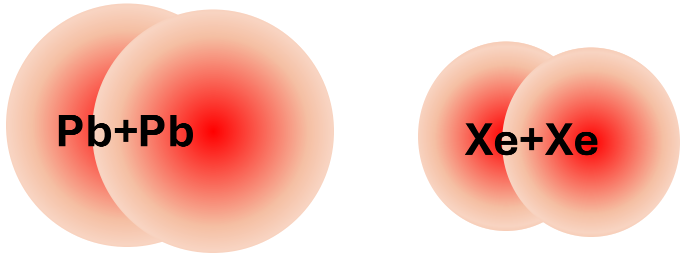

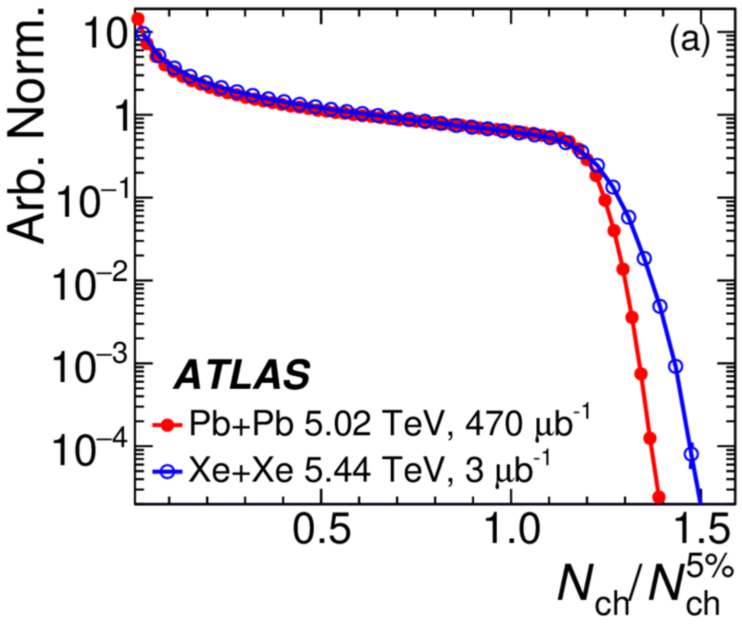

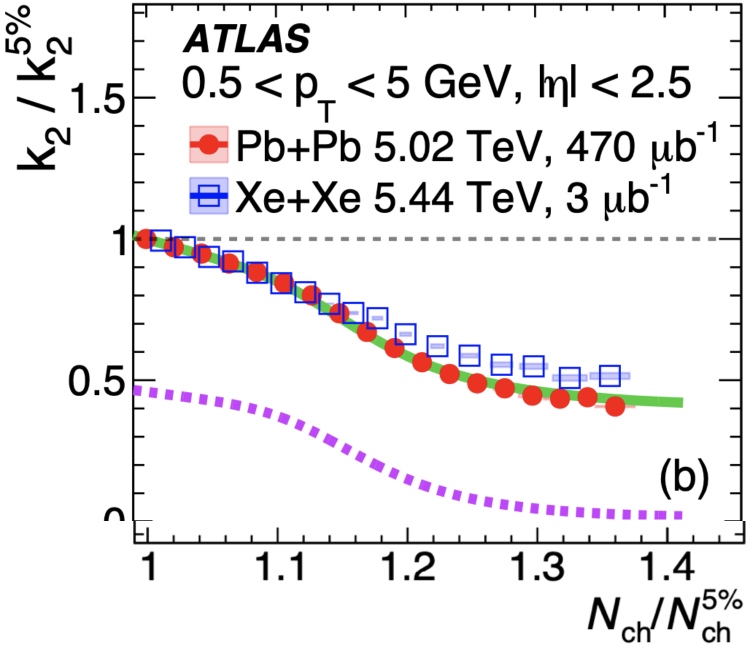

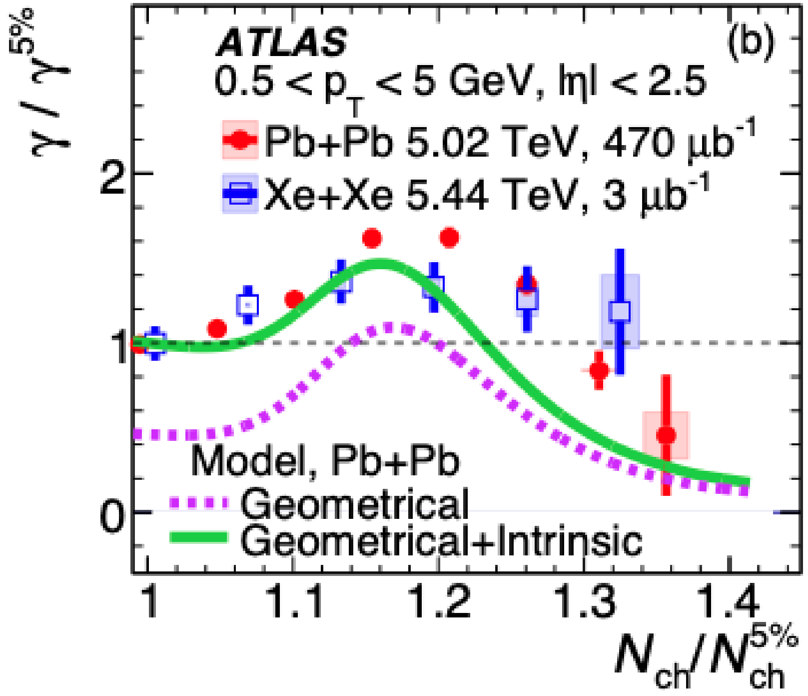

- Smaller System ⇒ Larger Smearing in Nch ⇒ UCC behavior from Geometrical suppression milder

Outlook I: Effect of System Size

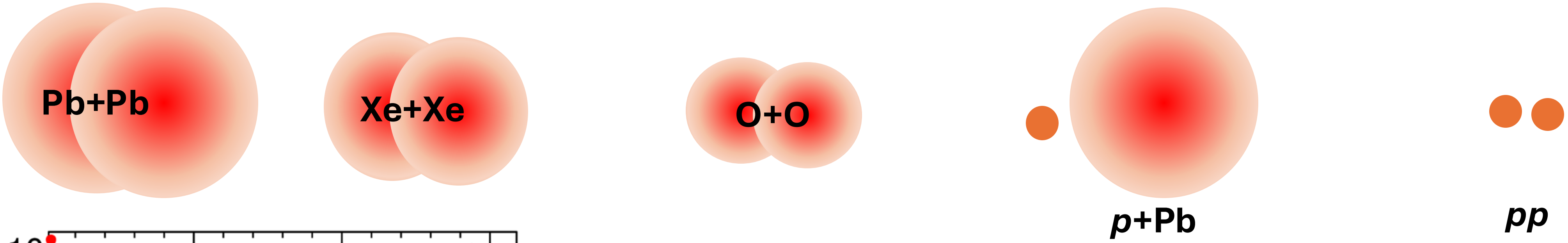

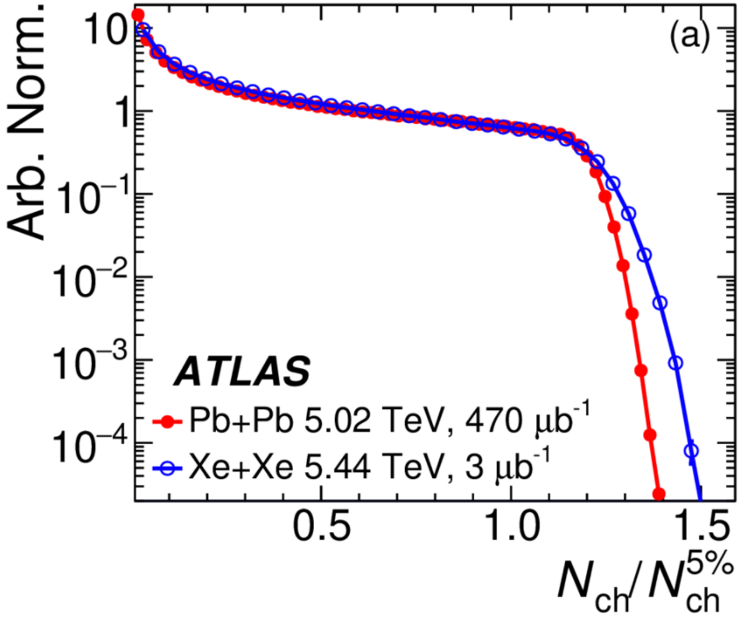

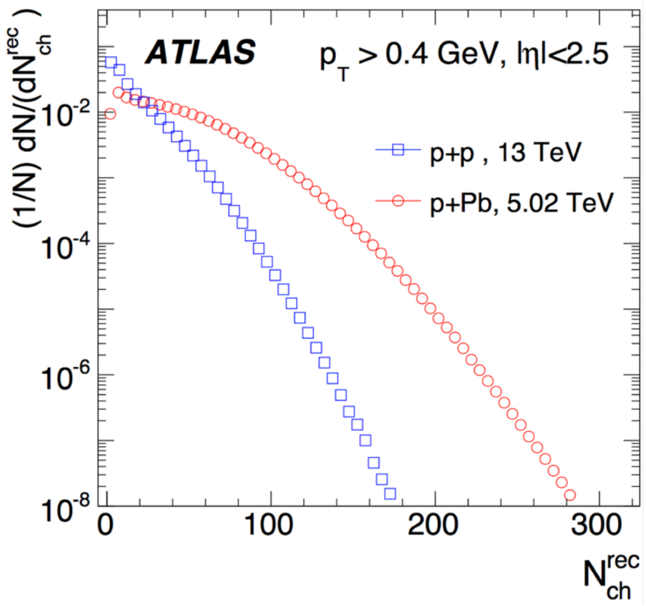

- Smaller System ⇒ Larger Smearing in Nch ⇒ UCC behavior from Geometrical suppression milder
- Similar analysis in smaller systems would test the limits on experimental disentanglement of Geometrical and Intrinsic components.

Prospects to study $\sqrt{s_{NN}}$ evolution of Geometrical and Intrinsic components of [p_T] fluctuations at STAR?

And many more…..

Exciting times ahead with using this novel approach to understand initial state fluctuations better!!

Thank You..

Backup

$$\gamma = \frac{\langle c_3 \rangle}{\langle c_2 \rangle^{3/2}}$$

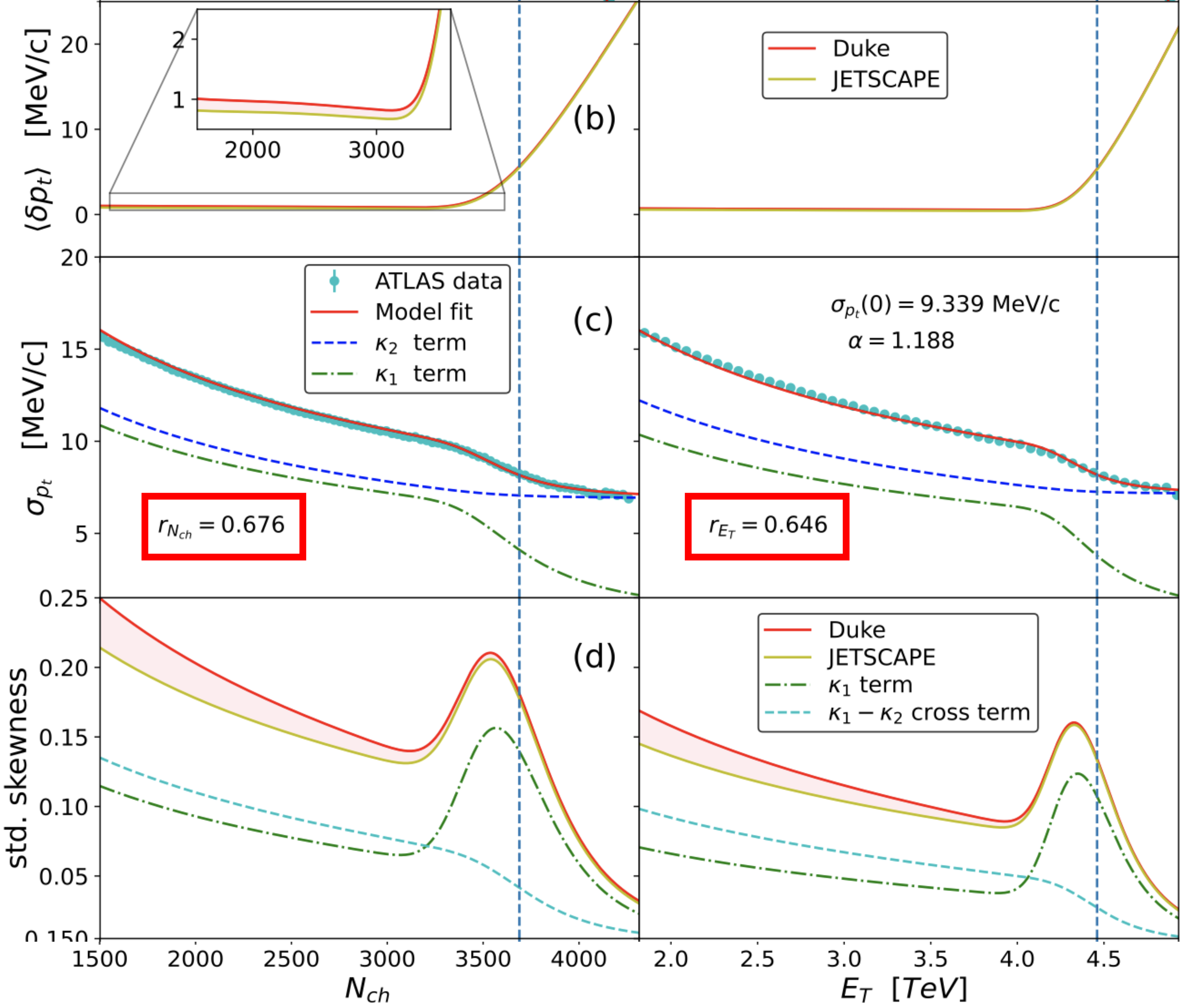

Samanta et. al, PRC109, L051902 (2024)

Constraining c_S^2 using $\langle [p_T] \rangle$

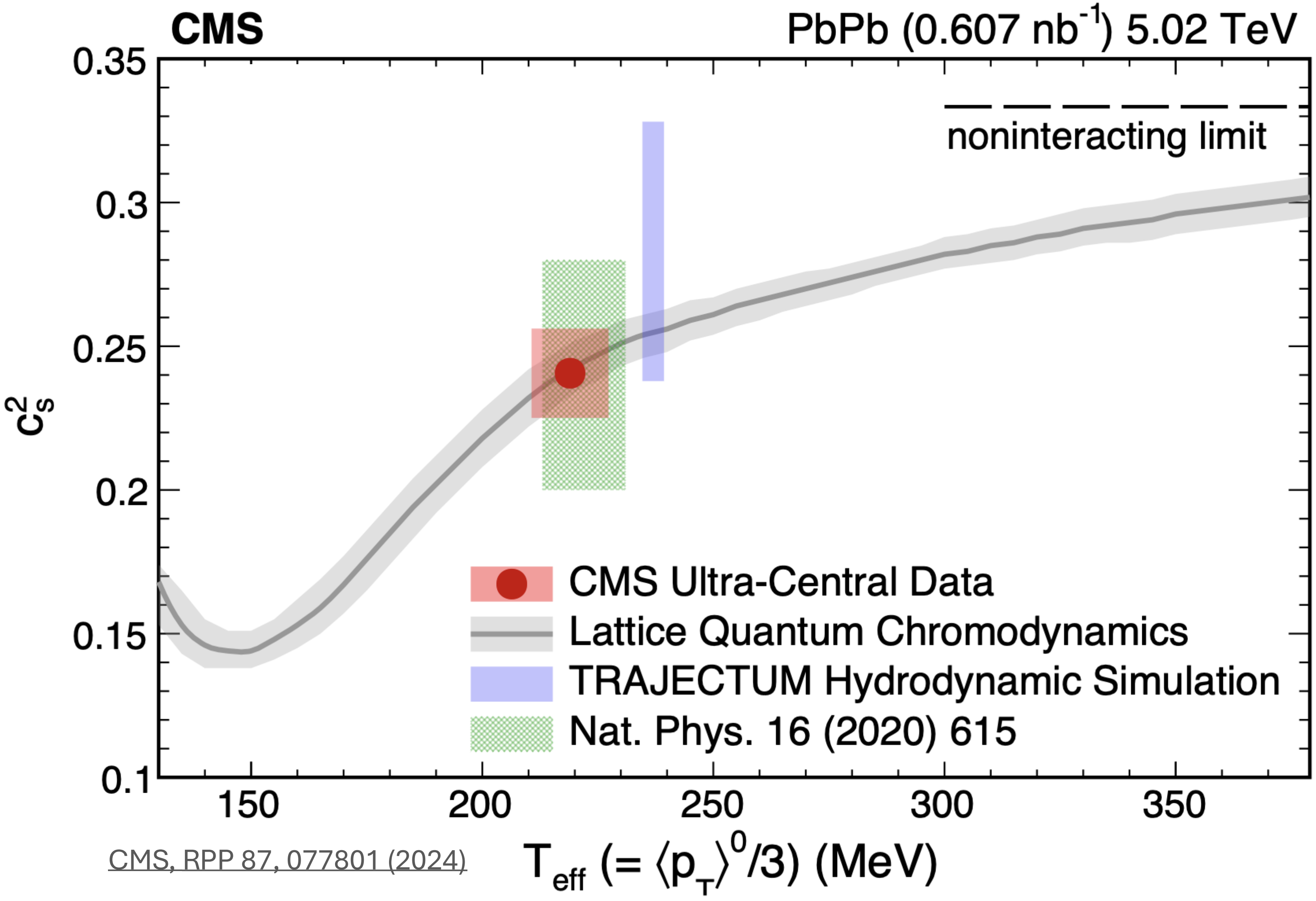

CMS, RPP 87, 077801 (2024)

- The value of c_s^2 extracted by CMS is consistent with Lattice QCD calculations at an effective temperature of about 220 MeV with small systematic error.
- UCC measurement of $\langle [p_T] \rangle$ provides direct information on c_s^2 of QGP.

Caveat: Dependence of extracted c_S^2 on Event-Class

ALICE-PUBLIC-2024-002

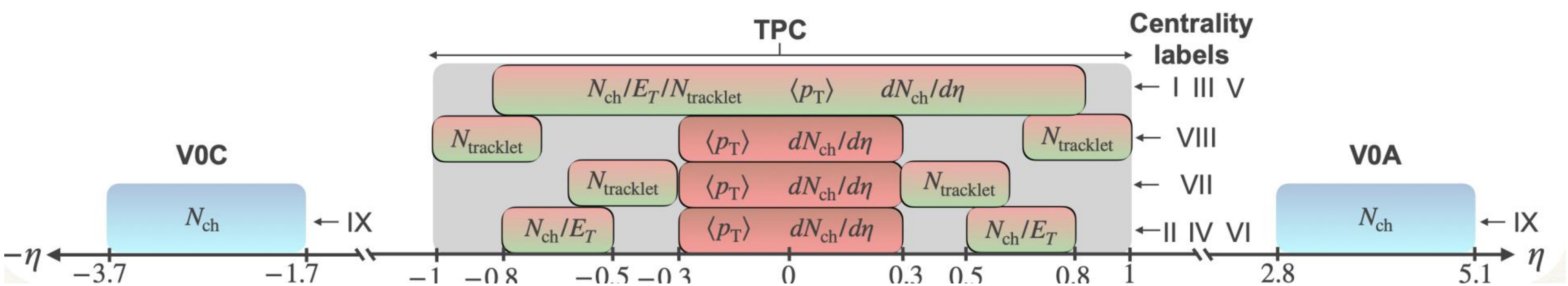

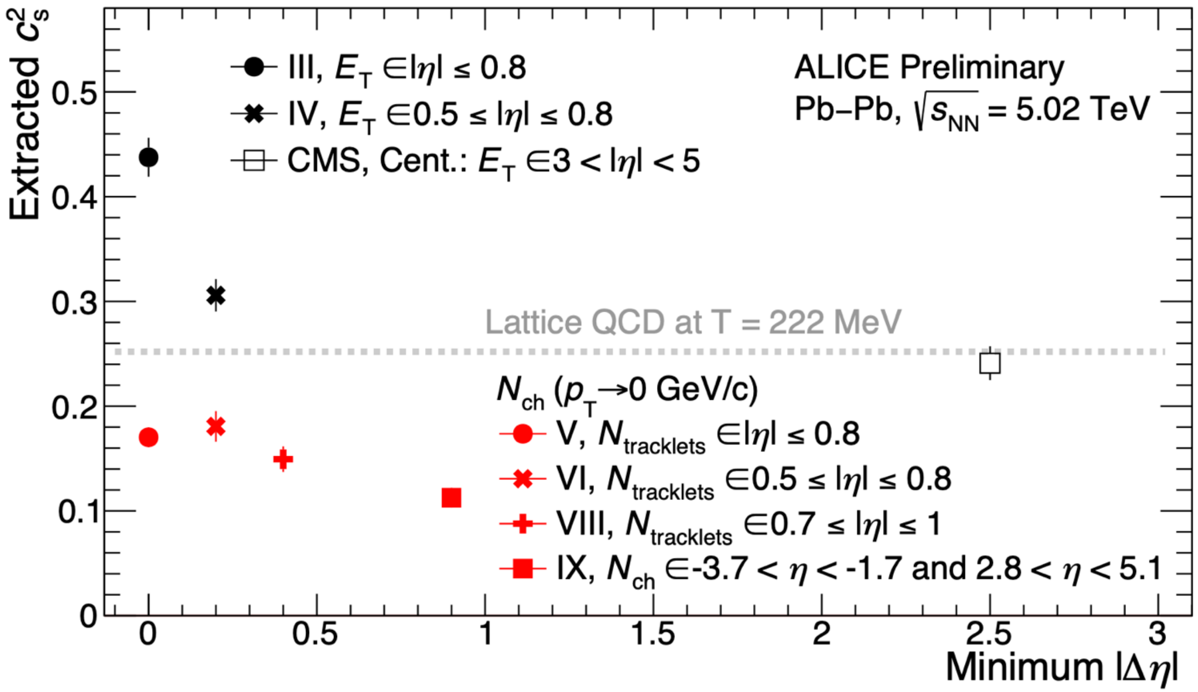

Observable	Label	Centrality estimation	$\langle p_T \rangle$ and $\langle dN_{ch}/d\eta \rangle$	η gap
N_{ch} in TPC	I	$\|\eta\| \leq 0.8$	$\|\eta\| \leq 0.8$	0
	II	$0.5 \leq \|\eta\| \leq 0.8$	$\|\eta\| \leq 0.3$	0.3
E_T in TPC	III	$\|\eta\| \leq 0.8$	$\|\eta\| \leq 0.8$	0
	IV	$0.5 \leq \|\eta\| \leq 0.8$	$\|\eta\| \leq 0.3$	0.3
$N_{tracklets}$ in SPD	V	$\|\eta\| \leq 0.8$	$\|\eta\| \leq 0.8$	0
	VI	$0.5 \leq \|\eta\| \leq 0.8$	$\|\eta\| \leq 0.3$	0.3
Silicon Pixel Detector	VII	$0.3 < \|\eta\| \leq 0.6$	$\|\eta\| \leq 0.3$	0
	VIII	$0.7 \leq \|\eta\| \leq 1$	$\|\eta\| \leq 0.3$	0.4
N_{ch} in V0	IX	$-3.7 < \eta < -1.7 + 2.8 < \eta < 5.1$	$\|\eta\| \leq 0.8$	1.7

- ALICE: The extracted c_S^2 depends on η selection of particles and event-class. c_S^2 for E_T based measurements larger
- Particle production in mid-rapidity differs from those in forward-rapidity ⇒ Centrality Fluctuations
- In addition, measured $[p_T]$ also expected to have decorrelation effects.